

Matrix elements of Lorentzian Hamiltonian constraint in loop quantum gravityEmanuele Alesci,^{1,*} Klaus Liegener,^{2,†} and Antonia Zipfel^{2,‡}¹*Institut Fizyki Teoretycznej, Uniwersytet Warszawski, ul. Hoża 69, 00-681 Warszawa, Poland, EU*²*Universität Erlangen, Institut für Theoretische Physik III, Lehrstuhl für Quantengravitation Staudtstrasse 7, D-91058 Erlangen, Germany*

(Received 29 July 2013; published 25 October 2013)

The Hamiltonian constraint is the key element of the canonical formulation of loop quantum gravity (LQG) coding its dynamics. In Ashtekar-Barbero variables it naturally splits into the so-called Euclidean and Lorentzian parts. However, due to the high complexity of this operator, only the matrix elements of the Euclidean part have been considered so far. Here we evaluate the action of the full constraint, including the Lorentzian part. The computation requires heavy use of $SU(2)$ recoupling theory and several tricky identities among n - j symbols are used to find the final result: these identities, together with the graphical calculus used to derive them, also simplify the Euclidean constraint and are of general interest in LQG computations.

DOI: [10.1103/PhysRevD.88.084043](https://doi.org/10.1103/PhysRevD.88.084043)

PACS numbers: 04.60.Pp

I. INTRODUCTION

In the Hamiltonian formulation general relativity (GR) is completely governed by the diffeomorphism and Hamiltonian constraints. For many years the complicated structure of these constraints prevented a quantization of the theory, until Ashtekar [1] suggested to replace the “old” metric variables by connections and tetrads. Indeed in these variables GR resembles other gauge theories, like Yang-Mills theory, whereupon one encounters an $SU(2)$ -Gauss constraint in addition to diffeomorphism and Hamiltonian constraints. This formulation was further improved by Barbero [2] and serves today as the classical starting point of loop quantum gravity (LQG) [3–5].

LQG follows the Dirac quantization program [6] for constrained systems, i.e. one introduces a preliminary kinematical Hilbert space on which the constraints can be represented by operators and then seeks the kernel of these operators defining the physical Hilbert space. The Gauss constraint is solved by introducing a so called “spin network” basis [7], naturally leading to a combinatorial discrete structure of space-time similar to the one proposed by Penrose [8], while the diffeomorphism constraint is solved by considering equivalence classes of spin networks under diffeomorphisms denoted “s-knots” [9].

A major obstacle for completing the canonical quantization program in LQG is the implementation of the Hamiltonian constraint S . The difficulties are mainly caused by the nonpolynomial structure of S and the weight factor $1/\sqrt{\det(q)}$ determined by the intrinsic metric $q := q_{ab}$ on the initial hypersurface Σ . In fact, Ashtekar [1] was motivated by the observation that the Hamiltonian constraint can be cast into a polynomial form when the metric

variables are replaced by triads and *complex* connections. Even though this simplifies the constraint one has to deal instead with difficult reality conditions. This reality structure is trivial when the theory is formulated in *real* connection variables as suggested by Barbero [2]. Unfortunately, the constraint is nonpolynomial in these variables. It was then proposed to absorb the weight $1/\sqrt{\det(q)}$ in the lapse function. But it turned out [10] that this density weight is crucial in order to obtain a finite, background independent operator.

After many efforts [11], Thiemann [12] discovered that both problems, the nonpolynomiality and the appearance of the weight factor, can be solved by expressing the inverse triads through the Poisson bracket of volume and connections (“Thiemann trick”). This trick made it possible to construct a finite, anomaly-free operator that corresponds to the nonrescaled Hamiltonian constraint [4,12,13] and acts by changing the underlying graph of the spin networks. The formal solution [13] to this constraint is superpositions of s-knot states with “dressed nodes,” which are nodes with a spiderweblike structure. Criticism appeared [14] mostly concerning the “ultralocal” character of the construction and regularization ambiguities. However, until now, this is the only known scheme able to realize an anomaly-free quantization of the Dirac algebra at least on shell.

This construction is at the heart of many other approaches within canonical LQG, such as the master constraint program [15], algebraic quantum gravity (AQG) [16], most recent models with matter [17–19], and symmetry reduced models like loop quantum cosmology [20,21]. Also the covariant approach (spin-foam models) [22] is motivated by the idea of realizing the “time evolution” generated by a graph-changing Hamiltonian [23]. In fact, it is hoped that the spin-foam model might provide a physical scalar product for canonical LQG (see e.g. [24]). The attempt to match both approaches (not only

*Emanuele.Alesci@fuw.edu.pl

†Klaus.Liegener@gravity.fau.de

‡antonia.zipfel@gravity.fau.de

heuristically) has led to new regularization schemes for the Hamiltonian constraint [25,26] and also to the discovery of new physical states in the canonical model [27].

Despite its central role for LQG the action of S has been analyzed explicitly in only very few examples [27–29] and these are confined to the Euclidean part of the constraint only. This is mainly due to two reasons: first the presence of the volume operator [30,31] and second the nontrivial recoupling of $SU(2)$ irreducible representations. The volume operator in LQG has been studied intensively under both the canonical [32–34] and the covariant perspective [35]. Yet, the matrix elements are getting very complicated with the more edges involved so that one has to apply numerical methods [36,37] or semiclassical analysis [38,39] to evaluate them. The second difficulty appears due to the regularization of the connections by holonomies. The corresponding operators act by multiplication which produces several Clebsh–Gordan decompositions and modifications to the intertwiners between $SU(2)$ representations at the nodes.

In this paper we explicitly compute the matrix elements of the *full* Lorentzian constraint in the Thiemann prescription for trivalent nodes. The final result still depends on the matrix elements of the volume which are unknown in closed form, but in principle computable. In the course of the evaluation several recoupling identities will be proven, which greatly simplify the final result and are expected to be useful in all the computations involving curvature loops or the “Thiemann trick.” The resulting compact formula presented here opens the possibility to test the implementation of the constraint by simulations, analyze the behavior of S in a large j limit, or further develop the methods of [27].

The article is organized as follows. In Sec. II Thiemann’s construction for the Euclidean and Lorentzian term is briefly reviewed and in Sec. III the main recoupling identities are introduced that will then be applied in Sec. IV to the Euclidean constraint leading to a new and very compact expression for it. Finally in Sec. V, we present the matrix elements of the Lorentzian part. Section VI is left for concluding remarks and two appendixes with further details on n - j symbols and the volume operator are included to make the manuscript self-contained.

II. HAMILTONIAN CONSTRAINT

A. Classical constraint

Let e_a^i be a triad on a smooth, spatial hypersurface Σ defining the intrinsic metric $q_{ab} = \delta_{ij} e_a^i e_b^j$. Here, $a, b = 1, 2, 3$ are tensorial and $i, j = 1, 2, 3$ are $\mathfrak{su}(2)$ indices. In the following, Γ_a^i denotes the spin-connection associated with e_a^i and K_{ab} the extrinsic curvature. Given $K_a^i := \text{sgn}(\det(e_c^j)) e_i^b K_{ab}$, it can be shown that the densitized inverse triad $E_i^a := \sqrt{\det(q)} e_i^a$ and $A_a^i := \Gamma_a^i + \gamma K_a^i$ form a canonical conjugated pair,

$$\{A_a^i(x), E_j^b(y)\} = \kappa \delta_j^i \delta_a^b \delta^{(3)}(x, y), \quad (1)$$

where γ is a real nonzero parameter and $\kappa = \frac{8\pi G}{c^3} \gamma$. If F_{ab} denotes the curvature of A and s the signature of the space-time metric then the classical Hamiltonian constraint is of the form

$$S = \frac{1}{\sqrt{\det(q)}} \text{Tr}\{(F_{ab} - (\gamma^2 - s)[K_a, K_b])[E^a, E^b]\}. \quad (2)$$

According to [12], the square root in (2) can be absorbed by using Poisson brackets of the connection A with the volume,

$$V := V(\Sigma) = \int_{\Sigma} dx^3 \sqrt{\det(q)}, \quad (3)$$

and the integrated curvature,

$$K := \int_{\Sigma} dx^3 E_j^a K_a^j. \quad (4)$$

More explicitly, inserting

$$\frac{[E^a, E^b]^i}{\sqrt{\det(q)}} = -\frac{2}{\kappa} \epsilon^{abc} \{A_c^i(x), V\} \quad \text{and} \quad K_a^i = \frac{1}{\kappa} \{A_a^i(x), K\} \quad (5)$$

in (2) yields

$$H = \frac{2}{\kappa} \epsilon^{abc} \text{Tr}(F_{ab} \{A_c, V\}) \quad (6)$$

and

$$T := S - H = (s - \gamma^2) \frac{4}{\kappa^3} \epsilon^{abc} \text{Tr}(\{A_a, K\} \{A_b, K\} \{A_c, V\}), \quad (7)$$

where S was split into an Euclidean part H and remaining constraint T , which vanishes for $\gamma^2 = 1$ and $s = 1$. The second part (7) can be further modified by expressing K through the “time” derivative of the volume:

$$K = -\frac{1}{\kappa \gamma} \left\{ V, \int_{\Sigma} dx^3 H \right\}. \quad (8)$$

Thus S is completely determined by the connection A , the curvature F , and the volume V all of which have well-defined operator analogues in LQG.

B. Quantization

Prior to quantization the local expressions (6) and (7) must be smeared and regularized. That is to say the connection and curvature of the integrated constraint $S[\mathcal{N}] := \int_{\Sigma} N(x) S(x)$ are replaced by holonomies along edges and loops, respectively. The properties of the operator depend highly on the chosen regularization and up to now there are several different models on the market (see e.g. [3,12,26]). Here, we follow the original proposal [12] because it is

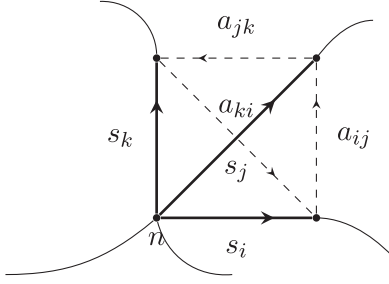


FIG. 1. An elementary tetrahedron $\Delta \in T$ constructed by adapting it to a graph Γ .

comparatively easy and leads to anomaly-free and finite operators.

Since the Euclidean constraint $H[N]$ depends linearly on the volume and the volume operator is acting locally on the nodes, it suffices to construct a regularization in the neighborhood of a node n in a given graph Γ and then extend it to all of Σ . Let s_l be a segment of an edge e_l incident at n and α_{IJ} the loop generated by s_I and s_J ; we mean $\alpha_{IJ} = s_I \circ \alpha_{IJ} \circ s_J^{-1}$ where α_{IJ} is a semianalytic arc which only intersects with Γ in the endpoints of s_I and s_J (see Fig. 1). In this way, any three (nonplanar) edges e_I , e_J , and e_K incident at n constitute an *elementary tetrahedron* Δ_{IJK} . Starting with Δ_{IJK} one can now construct seven additional tetrahedra (see [12] for details), such that the eight tetrahedra including Δ_{IJK} cover a neighborhood¹ of n . Afterwards this is extended to a full triangulation¹ $\mathfrak{T}(I, J, K)$ of Σ and $H[N]$ is decomposed into $\sum_{\Delta \in \mathfrak{T}} H_{\Delta}[N]$.

On the elementary tetrahedron Δ_{IJK} the connection A and the curvature F are regularized as usual by smearing along s_K and α_{IJ} , respectively, so that the regularized constraint is defined by

$$H_{\Delta_{IJK}}[N] := \sum_{i,j,k \in \{I,J,K\}} \frac{2}{3\kappa} N(n) \epsilon^{ijk} \text{Tr}[h_{\alpha_{ij}} h_{s_k} \{h_{s_k}^{-1}, V\}], \quad (9)$$

where h_s is the holonomy along side s and $N(n)$ is the value of the lapse function $N(x)$ at n . In the article [29] it was proposed to generalize this by considering holonomies in an arbitrary irrep m that yields

$$H_{\Delta_{IJK}}^m[N] := \sum_{i,j,k \in \{I,J,K\}} \frac{N(n)}{N_m^2 \kappa} \epsilon^{ijk} \text{Tr}[h_{\alpha_{ij}}^{(m)} h_{s_k}^{(m)} \{h_{s_k}^{(m)}, V\}], \quad (10)$$

with the normalization factor $N_m^2 = (2m+1)m(m+1)$. At this point, the quantization of (10) is straightforward. Its action on a cylindrical function T_s on a spin net s with underlying graph Γ is

¹Note, for each triple of edges adjacent to a node one constructs an *independent* triangulation.

$$\hat{H}[N]T_s = \frac{i}{N_m^2 \kappa l_p^2} \sum_{n \in \Gamma} \frac{8N(n)}{E(n)} \times \sum_{n(\Delta)=n} \epsilon^{ijk} \text{Tr}(h_{\alpha_{ij}}^{(m)} h_{s_k}^{(m)} [h_{s_k}^{(m)}, \hat{V}])T_s. \quad (11)$$

The first sum is running over all nodes of Γ and the second over all elementary tetrahedra. l_p is the Planck length. Because every vertex is surrounded by 8 tetrahedra, the smearing of H in the neighborhood of n yields 8 times the same factor. Apart from that, at an m -valent vertex n there are $E(n) := \binom{m}{3}$ elementary tetrahedra each of which determines an adapted triangulation. Therefore we need to divide by $E(n)$ to avoid overcounting.

A huge advantage of the operator defined above is that it is anomaly free, i.e. that the commutator of two constraints \hat{H} is vanishing up to diffeomorphisms. This is mainly due to the behavior of the volume which is vanishing on coplanar nodes.² But, in fact, H only generates such nodes (see Fig. 2) so that a second Hamiltonian acts again only on the “old” ones.

The remaining part of the constraint $T[N]$ can be quantized similarly. However, the regularization is a bit more involved because the extrinsic curvature must be regularized separately. In principle T adds two new links each of which is created by one operator $\hat{K} := \frac{i}{l_p^2 \gamma} [\hat{V}, \hat{H}[1]]$. To insure that the full constraint is still anomaly free, only coplanar nodes should be generated. That means, it must never happen that the two new links have a common intersection. Because \hat{H} is acting locally the second extrinsic curvature should be therefore regulated along tetrahedra lying inside of the first ones (see Fig. 2). The holonomies in T can be regulated as above such that finally

$$\hat{T}[N]T_s = \frac{2i(s - \gamma^2)}{N_m^2 \kappa l_p^6} \sum_{n \in \Gamma^{(0)}} \frac{8N(n)}{E(n)} \times \sum_{n(\Delta)=n} \epsilon^{ijk} \text{Tr}(h_{s_i}^{(m)} [h_{s_i}^{(m)}, \hat{K}] h_{s_j}^{(m)}) \times [h_{s_j}^{(m)}, \hat{K}] h_{s_k}^{(m)} [h_{s_k}^{(m)}, \hat{V}] T_s. \quad (12)$$

In Eqs. (11) and (12) the triangulation \mathfrak{T} serves as a regulator. This regularization dependence can be removed by using a suitable operator topology.³

²This is only true for the version defined by Ashtekar and Lewandowski [31], not the one introduced by Smolin and Rovelli [30].

³On diffeomorphism invariant states $\phi \in \mathcal{H}_{\text{diff}} \subset \mathcal{H}_{\text{kin}}^*$ the regulator dependence drops out trivially because two operators \hat{S} and \hat{S}' that are related by a refinement of the triangulation differ only in the size of the loops. This implies $\langle \phi, \hat{S}\psi \rangle = \langle \phi, \hat{S}'\psi \rangle$ (see [12] for details).

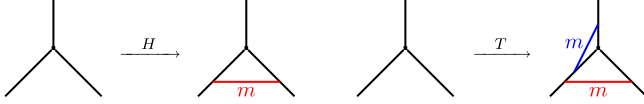


FIG. 2 (color online). The Euclidean constraint H creates a new link (red line) joining two edges at the same vertex due to the regularization of the curvature. On the right-hand side the principal action of T is visualized: The red link is created by the first extrinsic curvature while the blue one is created by the second curvature operator that is regularized along a tetrahedron lying inside of the first one.

III. COMPUTATIONAL TOOLS

In this section the tools for computing the matrix elements of the Hamiltonian constraint are introduced and some identities, which are important for the latter, are proven.

A. Graphical calculus

The evaluation of the above constraint is mainly based on recoupling theory of $SU(2)$. In this context it has proven beneficial to work with graphical methods. The calculus

that is used in this article was introduced in [27] and provides an extension of the methods in [40] that is especially useful in LQG because it incorporates an easy treatment of (nontrivial) group elements.

1. Basic definitions

In the following small Latin letters represent irreducible representations $j, \dots \in \frac{1}{2}\mathbb{N}$ while Greek ones, $\alpha, \dots = -j, -j+1, \dots, j$, are magnetic numbers. A state $|j, \alpha\rangle$ in the Hilbert space \mathcal{H}_j is visualized by $\overrightarrow{j, \alpha}$, the adjoint $\langle j, \alpha|$ is drawn as $\overleftarrow{j, \alpha}$ and a representation matrix $[R^j(g)]^\alpha_\beta$ with $g \in SU(2)$ is pictured as

$$\overrightarrow{\alpha} \xrightarrow{j, g} \overrightarrow{\beta}.$$

Two lines carrying the same representation

can be either connected by taking the scalar product, $\overrightarrow{j, \alpha} \overleftarrow{j, \alpha} = \sum_{\alpha=-j}^j \langle j, \alpha | j, \alpha \rangle$, or by contraction with the $2j$ symbol

$$\overrightarrow{\alpha} \xrightarrow{j} \overleftarrow{\beta} = \overleftarrow{\alpha} \xrightarrow{j} \overrightarrow{\beta} = \begin{pmatrix} j \\ \beta & \alpha \end{pmatrix} = (-1)^{j-\alpha} \delta_{\alpha, -\beta}. \quad (13)$$

This two-valent intertwiner defines an isometry between the vector representation (\rightarrow , tip) and the adjoint representation (\leftarrow , feather) whereby the transformations

$$\sum_{\beta} \begin{pmatrix} j \\ \beta & \alpha \end{pmatrix} |j, \beta\rangle = \langle j, \alpha| \quad \text{and} \quad \sum_{\beta} \begin{pmatrix} j \\ \alpha & \beta \end{pmatrix} \langle j, \beta| = |j, \alpha\rangle$$

are graphically encrypted in $\overrightarrow{\alpha} \xrightarrow{j} \overleftarrow{\beta} = \overrightarrow{\alpha} \xrightarrow{j} \overleftarrow{\beta}$ and $\overleftarrow{\alpha} \xrightarrow{j} \overrightarrow{\beta} = \overleftarrow{\alpha} \xrightarrow{j} \overrightarrow{\beta}$. The second identity can be derived from the first one using

$$\overleftarrow{\alpha} \xrightarrow{j} \overrightarrow{\beta} = \sum_{\tilde{\alpha}=-j}^j \begin{pmatrix} j \\ \alpha & \tilde{\alpha} \end{pmatrix} \begin{pmatrix} j \\ \beta & \tilde{\alpha} \end{pmatrix} = \delta_{\beta}^{\alpha} := \overleftarrow{\alpha} \xrightarrow{j} \overrightarrow{\beta}. \quad (14)$$

Note, the inner direction of (13) is crucial here since it indicates the order of the magnetic indices that differ by a sign when it is interchanged due to $(-)^{j+\alpha} = (-)^{2j}(-)^{j-\alpha}$ and $(-)^{2(j-\alpha)} = 1$. Consequently,

$$\overrightarrow{\alpha} \xrightarrow{j} \overleftarrow{\beta} = \overleftarrow{\beta} \xrightarrow{j} \overrightarrow{\alpha} = (-1)^{2j} \overrightarrow{\alpha} \xrightarrow{j} \overleftarrow{\beta} = (-1)^{2j} \overleftarrow{\beta} \xrightarrow{j} \overrightarrow{\alpha}.$$

Using (13) and the properties of Wigner matrices it is also straightforward to prove the following identity:

$$R^\beta_\alpha(g^{-1}) = (-1)^{\alpha-\beta} R^{-\alpha}_{-\beta}(g) = \overline{R^\alpha_\beta(g)}$$

$$\overleftarrow{\alpha} \xrightarrow{j} \overrightarrow{\beta} = \overleftarrow{\alpha} \xrightarrow{j} \overrightarrow{\beta} = \overleftarrow{\alpha} \xrightarrow{j} \overrightarrow{\beta}. \quad (15)$$

2. Recoupling

The basic building blocks of recoupling theory are the $3j$ symbols

$$\begin{pmatrix} a & b & c \\ \alpha & \beta & \gamma \end{pmatrix} \equiv \begin{array}{c} \uparrow a \\ + \\ \swarrow b \quad \searrow c \end{array} = \begin{array}{c} \Uparrow a \\ + \\ \swarrow b \quad \searrow c \end{array} \quad (16)$$

that arise from coupling two irreps a and b :

$$(R^a(g))^\alpha_{\tilde{\alpha}} (R^b(g))^\beta_{\tilde{\beta}} = \sum_{c=|a-b|}^{a+b} (2c+1) \sum_{\gamma, \tilde{\gamma}=-c}^c \begin{pmatrix} a & b & c \\ \alpha & \beta & \gamma \end{pmatrix} \begin{pmatrix} a & b & c \\ \tilde{\alpha} & \tilde{\beta} & \tilde{\gamma} \end{pmatrix} \overline{(R^c(g))^\gamma_{\tilde{\gamma}}}$$

$$\begin{array}{c} \xrightarrow{a} \\ \xrightarrow{b} \end{array} \begin{array}{c} \rightarrow \\ \rightarrow \end{array} = \sum_{c=|a-b|}^{a+b} (2c+1) \begin{array}{c} \Uparrow a \\ + \\ \swarrow b \quad \rightarrow c \\ - \\ \searrow a \quad \swarrow b \end{array} \quad (17)$$

As the tensor product $\mathcal{H}_a \otimes \mathcal{H}_b$ decomposes into $\bigoplus_{c=|a-b|}^{a+b} \mathcal{H}_c$, a $3j$ symbol (16) is vanishing if (a, b, c) are not compatible, i.e. if they do not obey $|a - b| \leq c \leq a + b$, and if $\alpha + \beta + \gamma \neq 0$. Since $3j$'s are intertwiners (or equivariant maps) they commute with the group action. That means $[R^a(g)]^\alpha_{\alpha'} \iota^{\alpha'\beta\gamma} = \iota^{\alpha\beta'\gamma'} [R^b(g)]^\beta_{\beta'} [R^c(g)]^\gamma_{\gamma'}$ for any trivalent intertwiner $\iota^{\alpha\beta\gamma}$, which is encoded in

$$\begin{array}{c} \xrightarrow{a} \\ \rightarrow \end{array} \begin{array}{c} \rightarrow \\ \rightarrow \end{array} = \begin{array}{c} \rightarrow \\ \rightarrow \end{array} \begin{array}{c} \rightarrow \\ \rightarrow \end{array} \quad (18)$$

Apart from that, these symbols are invariant under an even permutation of columns and related by $(-1)^{a+b+c}$ for an odd permutation. For this reason one has to assign an orientation to the nodes labeling anticlockwise (+) and clockwise (-) order of the links [compare with (16)]. Another important symmetry is

$$\begin{pmatrix} a & b & c \\ \alpha & \beta & \gamma \end{pmatrix} = (-1)^{a+b+c} \begin{pmatrix} a & b & c \\ -\alpha & -\beta & -\gamma \end{pmatrix} \quad (19)$$

The trivalent intertwiners (16) are fundamental building blocks. All other intertwiners can be obtained from these. For example a node which has ingoing as well as outgoing links is constructed by multiplying with (13):

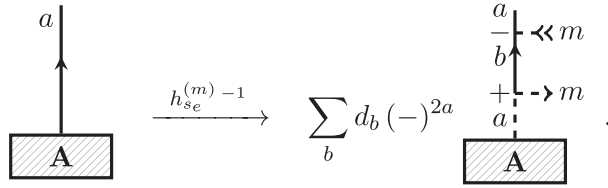
$$\begin{array}{c} \Uparrow a \\ + \\ \swarrow b \quad \searrow c \end{array} = (-1)^{a-\alpha} \begin{pmatrix} a & b & c \\ -\alpha & \beta & \gamma \end{pmatrix} := \begin{array}{c} \Uparrow a \\ + \\ \swarrow b \quad \searrow c \end{array} \quad (20)$$

This together with (19) proves the equivalence of a trivalent node whose links are all ingoing with one whose links are all outgoing, as was claimed in (16). Moreover, the intertwiner (20) is of importance when coupling two holonomies with opposed orientation. In this case one finds with (15) and $d_c \equiv 2c + 1$

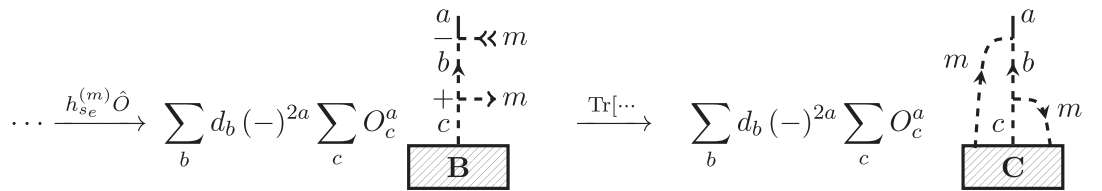
$$\begin{array}{c} \xrightarrow{a} \\ \xrightarrow{b} \end{array} \begin{array}{c} \rightarrow \\ \rightarrow \end{array} \stackrel{(15)}{=} \begin{array}{c} \xrightarrow{a} \\ \xleftarrow{b} \end{array} \begin{array}{c} \rightarrow \\ \rightarrow \end{array} = (-1)^{2a} \sum_{c=|a-b|}^{a+b} d_c \begin{array}{c} \Uparrow a \\ + \\ \swarrow b \quad \rightarrow c \\ - \\ \searrow a \quad \swarrow b \end{array} \quad (21)$$

(21) if they share (a part of) a solid edge. Instead, dashed parts can be modified arbitrarily or even removed (see below for examples) as long as they live at the same node.⁵

Nevertheless, solid parts can be transformed into dashed ones by the action of an operator as will be explained in the following example. Consider the action of $\text{Tr}[\dots h_{s_e}^{(m)} \hat{O} h_{s_e}^{(m)-1}]$ on a node A (box in the graphic below) where s_e is a part of an edge e emanating from the node and \hat{O} is an arbitrary operator not depending on a holonomy along s_e . To start with, the first holonomy $h_{s_e}^{(m)-1}$ is coupled to s_e via (21):



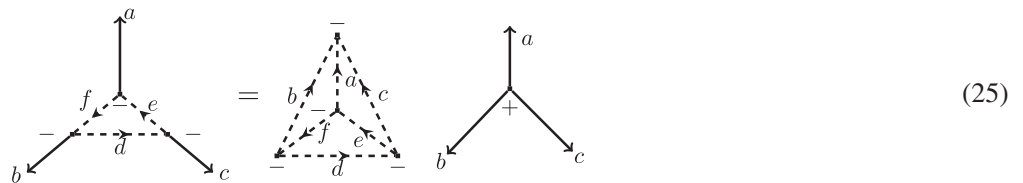
Here \rightarrow and \rightsquigarrow , being open ended lines with tips and arrows, represent the magnetic indexes of $h_{s_e}^{(m)-1}$ which are not contracted yet (note that in the whole article the index m is always used only as a spin, never as a magnetic number; magnetic indexes only appear with greek fonts). The operator \hat{O} will in general change the intertwiner, which now consists of A and the dashed edge a . After evaluating \hat{O} the holonomy $h_{s_e}^{(m)}$ is multiplied as the tip of $h_{s_e}^{(m)}$ is contracted with the feather of $h_{s_e}^{(m)-1}$ so that



The solid part b is turned into a dashed part since first of all going along s_e^{-1} and then along s_e pulls \rightsquigarrow back to the node and secondly the group element can be removed of $h_{s_e}^{(m)}$ and b due to (18). After all other components of the operator have been applied the trace can be closed merging the remaining \rightarrow and \rightsquigarrow .

B. Important identities

It will now be demonstrated how to work with the above calculus by means of specific examples, which will be important in what follows. A useful technique to simplify complicated couplings is to insert a resolution of identity at the intertwiner space. For example contracting the vertex on the left of this equation



with a trivalent vertex yields a tetrahedron that equals $\{ \begin{smallmatrix} a & b & c \\ d & e & f \end{smallmatrix} \}$. This relation in combination with (24) proves to be very handy for the evaluation of the following diagram:

⁵The only case where a solid line can be removed is when, through the coupling of other holonomies, the coloring of the edge is changed to the trivial representation.

$$\begin{aligned}
 & \stackrel{(24)}{=} \sum_{z_3} d_{z_3} (-)^{2z_1} (-)^{z_3+c+\tilde{m}} \left\{ \begin{matrix} z_1 & z_2 & \tilde{m} \\ c & z_3 & m \end{matrix} \right\} \\
 & \stackrel{(25)}{=} \sum_{z_3} d_{z_3} (-)^{2y} (-)^{a+b+c+\tilde{m}} \left\{ \begin{matrix} z_1 & z_2 & \tilde{m} \\ c & z_3 & m \end{matrix} \right\} \left\{ \begin{matrix} a & b & z_3 \\ m & z_1 & y \end{matrix} \right\}
 \end{aligned} \tag{26}$$

The signs arise from adjusting the orientation of edges and nodes. To apply (25) the orientation of the link z_3 in the second graphic has to be flipped and all nodes involved must be labeled by $-$ instead of $+$ that gives $(-)^{4z_3+2(y+m)}(-)^{a+b+z_3} = (-)^{2(y+m)}(-)^{a+b+z_3}$. Since $4j$ is an even integer for any spin j and $(-)^{2z_1} = (-)^{2(m+z_3)}$ because (z_1, z_3, m) are compatible, the final sign reduces to $(-)^{2y}(-)^{a+b+c+\tilde{m}}$.

Instead of interchanging m and \tilde{m} one could have also used (24) to move \rightarrow to the edge a before applying (25). Following this procedure one finds

$$= \sum_x d_x (-)^{x+y+z_1+z_2+m+b-a} \left\{ \begin{matrix} z_1 & z_2 & \tilde{m} \\ a & x & y \end{matrix} \right\} \left\{ \begin{matrix} x & b & c \\ m & z_2 & y \end{matrix} \right\}$$

$$\tag{27}$$

On the other hand, the basis must be changed at least 2 times if \rightarrow should be finally aligned to b . Thus,

$$= \sum_{\tilde{y}} d_{\tilde{y}} (-)^{2(a+y)} (-)^{b+\tilde{y}+\tilde{m}} \left\{ \begin{matrix} k & a & \tilde{y} \\ m & y & b \end{matrix} \right\} \left\{ \begin{matrix} z_2 & z_1 & \tilde{m} \end{matrix} \right\}$$

$$\tag{28}$$

where the sum over the resulting three $6j$'s [one from (25)] can be summarized in a $9j$ symbol⁶:

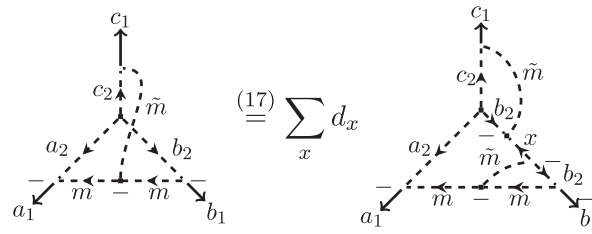
$$\left\{ \begin{matrix} a & f & r \\ d & q & e \\ p & c & b \end{matrix} \right\} := \sum_x d_x (-1)^{2x} \left\{ \begin{matrix} a & b & x \\ c & d & p \end{matrix} \right\} \left\{ \begin{matrix} c & d & x \\ e & f & q \end{matrix} \right\} \left\{ \begin{matrix} e & f & x \\ a & b & r \end{matrix} \right\}.$$

$$\tag{29}$$

It is often easier to follow the signs when one uses (17) [or (21)] and (25) instead of (24) as it is demonstrated in the subsequent example⁷:

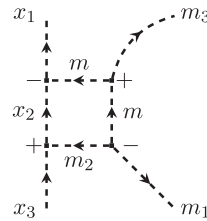
⁶See Appendix A for more details.

⁷Since in this specific case \tilde{m} is an integer, changing the orientation of the link \tilde{m} does not contribute a sign which is why there is no arrow assigned to the link.



Removing the line \tilde{m} between the upper link and the one on the right leads indeed to the same $6j$ as (24). After eliminating the legs labeled by \tilde{m} in the right diagram the link m is vanishing as well due to (24). The resulting $6j$'s can again be summed up to a $9j$:

Apart from the above examples, couplings of the form



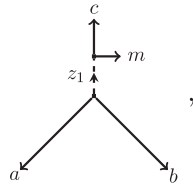
are encountered in the subsequent analysis. Coupling the link m_3 in a suitable way [here with (21)] yields

where (25) was utilized first to take away the two legs m_3 and afterwards x_2 .

C. Action of the volume

Even though the volume cannot be computed analytically for generic configurations, it is comparatively easy to calculate it for gauge-variant trivalent vertices transforming in a low spin. This is exactly the type of nodes that are of interest here. Nevertheless, we will not explicitly calculate these matrix elements in this section but only summarize some generic properties. More details can be found in Appendix B.

Noninvariant trivalent intertwiners can be treated as four-valent (invariant) ones, e.g.



where one leg, here m , does not correspond to a true edge but indicates in which representation the node is transforming. In a slight abuse of the conventions these open ends m are drawn as solid rather than dashed lines for better visibility. Whether a leg at the intertwiner corresponds to a part of a true edge or is indicating gauge variance follows from the context.

In general \hat{V} alters the intertwiner structure, so that

$$\hat{V} \begin{array}{c} c \\ \uparrow \\ z_1 \\ \swarrow \quad \searrow \\ a \quad b \end{array} \begin{array}{c} m \\ \rightarrow \end{array} := \sum_{z_2} V_{z_2}^{z_1}(a, b|c; m) \begin{array}{c} c \\ \uparrow \\ z_2 \\ \swarrow \quad \searrow \\ a \quad b \end{array} \begin{array}{c} m \\ \rightarrow \end{array} . \quad (32)$$

Note, the above definition of the matrix elements $V_{z_2}^{z_1}$ depends crucially on the order of the node as well as the orientation of the edges. Consider, for example, a node whose legs a and b are interchanged. Switching the legs back into the original position before acting with \hat{V} gives a sign $(-)^{z_1+a+b}$, while exchanging them after the volume has been applied yields $(-)^{z_2+a+b}$ so that $V_{z_2}^{z_1}(a, b|c; m) = (-)^{z_1-z_2} V_{z_2}^{z_1}(b, a|c; m)$.

IV. ACTION OF THE EUCLIDEAN CONSTRAINT

The action of the Euclidean constraint on trivalent nodes was determined for the first time in [28,29] using Temperley-Lieb algebras and recalculated in [27] by graphical methods similar to the one introduced above. In this section a powerful trick is presented that hugely simplifies this calculation.

A. Action on gauge-invariant trivalent vertices

For a single trivalent vertex with adjacent edges e_i, e_j, e_k the Euclidean constraint (11) reduces to

$$\frac{4i}{N_m^2 \kappa l_p^2} \epsilon^{ijk} \text{Tr}_m[(h_{\alpha_{ij}} - h_{\alpha_{ji}}) h_{s_k} [h_{s_k^{-1}}, V]], \quad (33)$$

where the Lapse $N(\mathfrak{n})$ was set to one and the subscript m in Tr_m indicates that the holonomies have spin m . Moreover, since $\text{Tr}_m[h_{\alpha_{ij}}] = \text{Tr}_m[(h_{\alpha_{ij}})^{-1}] = \text{Tr}_m[h_{\alpha_{ji}}]$ expression (33) reduces further to⁸

$$\frac{4i}{N_m^2 \kappa l_p^2} \epsilon^{ijk} \text{Tr}_m[(h_{\alpha_{ij}} - h_{\alpha_{ji}}) h_{s_k} V h_{s_k^{-1}}]. \quad (34)$$

To begin with, the holonomy $h_{s_k^{-1}}$ has to be coupled to the edge e_k which leads to a gauge-variant vertex because the magnetic indices are not contracted yet. Consequently,

$$V h_{s_k^{-1}} \begin{array}{c} j_k \\ \uparrow \\ \swarrow \quad \searrow \\ j_i \quad j_j \end{array} = V \sum_{c_1} d_{c_1} (-)^{2j_k} \begin{array}{c} c \\ \uparrow \\ - \leftarrow m \\ + \rightarrow m \\ j_k \\ \uparrow \\ \swarrow \quad \searrow \\ j_i \quad j_j \end{array} = \sum_{c_1, c_2} d_{c_1} (-)^{2j_k} V_{c_2}^{j_k}(j_i, j_j|c_1; m) \begin{array}{c} c \\ \uparrow \\ - \leftarrow m \\ + \rightarrow m \\ c_2 \\ \uparrow \\ \swarrow \quad \searrow \\ j_i \quad j_j \end{array} . \quad (35)$$

⁸This argument applies to *all* intertwiners so that the commutator can be always replaced by $h_{s_k} V h_{s_k^{-1}}$.

The action of the remaining holonomies in (34) can be simplified by
Theorem (loop trick)

$$\frac{1}{2}(h_{\alpha_{ij}} - h_{\alpha_{ji}})h_{s_k} = \epsilon(i, j, k) \sum_{\tilde{m} \in (2\mathbb{N}+1)} d_{\tilde{m}} (-)^{2m} \begin{array}{c} \uparrow \\ \leftarrow \tilde{m} \pm \\ \tilde{m} \mp \\ \triangleleft \quad \triangleright \\ m \end{array} \quad (36)$$

where $\epsilon(i, j, k) = 1$ if the edges e_i, e_j, e_k are ordered anticlockwise, otherwise it equals -1 .

Proof. The “free ends” of $(h_{\alpha_{ij}} - h_{\alpha_{ji}})h_{s_k}$ can be joined artificially by (21) which is graphically encoded in

$$(h_{\alpha_{ij}} - h_{\alpha_{ji}})h_{s_k} = \epsilon(i, j, k) \left(\begin{array}{c} \uparrow \\ \vdots \\ \triangleleft \quad \triangleright \\ m \end{array} - \begin{array}{c} \uparrow \\ \vdots \\ \triangleright \quad \triangleleft \\ m \end{array} \right) = \epsilon(i, j, k) \sum_{\tilde{m}} d_{\tilde{m}} (-)^{2m} \left(\begin{array}{c} \uparrow \\ \tilde{m} \pm \\ \tilde{m} \mp \\ \triangleleft \quad \triangleright \\ m \end{array} - \begin{array}{c} \uparrow \\ \tilde{m} \pm \\ \tilde{m} \mp \\ \triangleright \quad \triangleleft \\ m \end{array} \right).$$

Suppose $h_{ij} = [R^m(g)]^\mu_\nu$ then

$$\begin{aligned} \begin{array}{c} \tilde{m}, \gamma \\ \vdots \\ \nu \quad \mu \\ \triangleleft \quad \triangleright \\ m \end{array} &\equiv \sum_{\mu, \nu} \begin{pmatrix} \tilde{m} & m & m \\ \gamma & \nu & -\mu \end{pmatrix} (-1)^{m-\mu} [R^m(g^{-1})]^\nu_\mu \\ &= \sum_{\mu, \nu} (-1)^{2m+\tilde{m}} \begin{pmatrix} \tilde{m} & m & m \\ \gamma & -\mu & \nu \end{pmatrix} (-1)^{m-\nu} [R^m(g)]^{-\mu}_{-\nu} \\ &= (-1)^{\tilde{m}} \sum_{\mu, \nu} \begin{pmatrix} \tilde{m} & m & m \\ \gamma & \mu & -\nu \end{pmatrix} (-1)^{m-\nu} [R^m(g)]^\mu_\nu \equiv (-1)^{\tilde{m}} \begin{array}{c} \tilde{m}, \gamma \\ \nu \quad \mu \\ \triangleleft \quad \triangleright \\ m \end{array}. \end{aligned}$$

To pass from the first line to the second, relation (15) was invoked. The sign $(-)^{2m+\tilde{m}}$ originates from the permutation of the columns of the $3j$ symbol and is annihilated due to (19) in the last line.

Inserting this in the first equality proves the theorem.

As in the example on page 11, adding h_{s_k} to (35) transforms the solid line c_1 into a dashed line so that with (36) and $\tilde{\Sigma}_x := \sum_x d_x$ one obtains

$$\text{Tr}_m[(h_{\alpha_{ij}} - h_{\alpha_{ji}}) \cdots] = 2 \epsilon(i, j, k) \sum_{\substack{a, b, c_1; \\ m_1 \in (2\mathbb{N}+1)}} \sum_{c_2} (-)^{2b} V_{c_2}^{jk}(j_i, j_j | c_1; m)$$

(37)

$$= 2 \epsilon(i, j, k) \sum_{\substack{a, b, c_1; \\ m_1 \in (2\mathbb{N}+1)}} \sum_{c_2} V_{c_2}^{jk}(j_i, j_j | c_1; m) (-)^{j_j - b + c_2 - c_1} \begin{Bmatrix} m & m & m_1 \\ j_k & c_2 & c_1 \end{Bmatrix} \begin{Bmatrix} a & j_i & m \\ b & j_j & m \\ j_k & c_2 & m_1 \end{Bmatrix}$$

(38)

In (37) the sign $(-)^{2(j_k+m)}$ stemming from coupling $h_{s_{-1}}$ and from (36) is canceled by $(-)^{2m}$, which arises from coupling the part $h_{s_{-1}}$ of $h_{\alpha_{ij}}$, and by $(-)^{2a} = (-)^{2(b+j_k)}$ that is produced by the switch of the direction of a after coupling h_{s_i} . The dashed parts of the diagram are removed by first making use of (25) to get rid of the triangle (m, m, c_1) and then of (30). Parts of the signs resulting from these two moves were afterwards absorbed by an odd permutation of rows and columns of the $9j$ symbol.⁹

To obtain the full action of \hat{H} the above expression has to be contracted with ϵ^{ijk} so that

$$\hat{H} = \sum_{a,b} H_{ab}^{j_i j_j}(j_k) + \sum_{b,c} H_{bc}^{j_j j_k}(j_i) + \sum_{c,a} H_{ca}^{j_k j_i}(j_j)$$

with

$$H_{ab}^{j_i j_j}(j_k) = \frac{8i}{N_m^2 \kappa_l^2 p} \epsilon(i, j, k) \sum_{\substack{c_1; \\ m_1 \in (2\mathbb{N}+1)}} \sum_{c_2} V_{c_2}^{jk}(j_i, j_j | c_1; m) (-)^{j_i - b + c_2 - c_1} \begin{Bmatrix} m & m & m_1 \\ j_k & c_2 & c_1 \end{Bmatrix} \begin{Bmatrix} a & j_i & m \\ b & j_j & m \\ j_k & c_2 & m_1 \end{Bmatrix}. \quad (39)$$

As for the volume, it is crucial to respect the orientation of the nodes and edges in the above formula. For example,

$$\hat{H} = \sum_{a,b} H_{ba}^{j_j j_i}(j_k) + \cdots$$

Swapping the legs j_i and j_j back into the original position before applying \hat{H} generates a sign $(-)^{j_i + j_j + j_k}$ and switching them afterwards again contributes $(-)^{a+b+j_k} (-)^{a+j_i+m} (-)^{b+j_j+m}$ for the nodes and $(-)^{2(a+b+m)}$ for reorienting the loop so that in total¹⁰ $H_{ab}^{j_i j_j}(j_k) = H_{ba}^{j_j j_i}(j_k)$. This result seems to be astonishing at first sight since \hat{H} is antisymmetric. However, if

⁹See Appendix A for details.

¹⁰The same conclusion can be reached by directly analyzing Eq. (39).

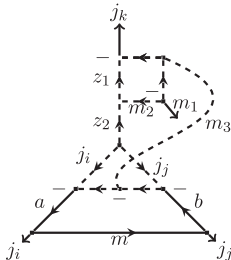
(j_i, a) and (j_j, b) are exchanged in the matrix element then α_{ij} changes its direction but also the legs of the nodes are twisted so that in total this is nothing else than a relabeling and therefore should not change the value.

B. Action on gauge-variant nodes

Below we will have to calculate the extrinsic curvature of gauge-variant nodes, which is why we also have to evaluate the action of \hat{H} on nodes of this kind (here: a trivalent one transforming in spin m_1). To start with we apply the following trick:

$$\begin{aligned}
 & \begin{array}{c} j_k \\ \uparrow \\ c_1 \xrightarrow{m_1} \\ \swarrow \quad \searrow \\ j_i \quad j_j \end{array} \xrightarrow{h_{s_k}^{(m)} h_{s_k}^{-1}} \sum_{z_2} (-)^{2j_k} \begin{array}{c} j_k \\ \uparrow \\ - \leftarrow m \\ z_1 \uparrow \\ + \rightarrow m \\ j_k \uparrow \\ c_1 \xrightarrow{m_1} \\ \swarrow \quad \searrow \\ j_i \quad j_j \end{array} \\
 & = \sum_{z_1, m_2} (-)^{2j_k} \begin{array}{c} j_k \\ \uparrow \\ - \leftarrow m \\ z_1 \uparrow \\ j_k \uparrow \xrightarrow{m_2} \leftarrow m \\ \swarrow \quad \searrow \\ c_1 \xrightarrow{m_1} \\ \swarrow \quad \searrow \\ j_i \quad j_j \end{array} = \sum_{z_1, m_2} (-)^{2(j_k+m_1)} (-)^{c_1+z_1+m_2} \left\{ \begin{array}{ccc} m & m_1 & m_2 \\ c_1 & z_1 & j_k \end{array} \right\} \begin{array}{c} j_k \\ \uparrow \\ - \leftarrow m \\ z_1 \uparrow \\ m_2 \leftarrow m \\ c_1 \xrightarrow{m_1} \\ \swarrow \quad \searrow \\ j_i \quad j_j \end{array} .
 \end{aligned} \tag{40}$$

Here, neither \rightarrow nor \leftarrow corresponds to true edges. Rather they indicate that the node is transforming in $\mathcal{H}_m \otimes \mathcal{H}_{m_1}$. Since the volume acts as a derivative operator and therefore only ‘‘grasps’’ true edges (see Appendix B), it is advisable to glue \rightarrow and \leftarrow together, taking advantage of (17) and (25). Instead of having to evaluate \hat{V} on the node with two open links, it is now possible to simply treat it as before acting on a node with just one open leg $m_2 \in \{|m - m_1|, \dots, m + m_1\}$. Together with(36) this yields

$$\begin{aligned}
 & \frac{1}{2} \text{Tr}_m [(\alpha_{ij} - \alpha_{ji}) h_{s_k} \hat{V} h_{s_k}^{-1}] \begin{array}{c} j_k \\ \uparrow \\ c_1 \xrightarrow{m_1} \\ \swarrow \quad \searrow \\ j_i \quad j_j \end{array} = \\
 & \epsilon(i, j, k) \sum_{\substack{z_1, m_2 \\ a, b}} \sum_{m_3 \in 2N+1} \sum_{z_2} (-)^{c_1+z_1+m_2+2b} \left\{ \begin{array}{ccc} m & m_1 & m_2 \\ c_1 & z_1 & j_k \end{array} \right\} V_{z_2}^{c_1} (j_i, j_j | z_1; m_2)
 \end{aligned}$$


The dashed parts can be simplified exerting (30) and (31) and the symmetries of $9j$'s:

$$\begin{aligned}
 & \begin{array}{c} j_k \\ \uparrow \\ z_1 \\ \uparrow \\ z_2 \\ \uparrow \\ c_2 \\ \uparrow \\ m_1 \\ \uparrow \\ m_2 \\ \uparrow \\ m_3 \\ \uparrow \\ j_i \quad j_j \\ \swarrow \quad \searrow \\ a \quad b \end{array} \quad \stackrel{(31)}{=} \quad \sum_{c_2} \tilde{(-)}^{2z_1} (-)^{z_2+m+m_1+m_2-c_2} \begin{Bmatrix} m_2 & z_1 & z_2 \\ m_1 & j_k & c_2 \\ m & m & m_3 \end{Bmatrix} \begin{array}{c} j_k \\ \uparrow \\ m_1 \\ \uparrow \\ z_2 \\ \uparrow \\ m_3 \\ \uparrow \\ j_i \quad j_j \\ \swarrow \quad \searrow \\ a \quad b \end{array} \\
 & \stackrel{(30)}{=} \quad \sum_{c_2} \tilde{(-)}^{2m} (-)^{j_i+a+m_1-m_2} \begin{Bmatrix} m_2 & z_1 & z_2 \\ m_1 & j_k & c_2 \\ m & m & m_3 \end{Bmatrix} \begin{Bmatrix} j_i & j_j & z_2 \\ a & b & c_2 \\ m & m & m_3 \end{Bmatrix} \begin{array}{c} j_k \\ \uparrow \\ c_2 \\ \uparrow \\ m_1 \\ \uparrow \\ a \quad b \end{array}
 \end{aligned}$$

With the remaining summands of H one can proceed similarly if the basis of the intertwiner is changed before the trace is evaluated such that \rightarrow is always assigned to the edge facing the loop. The full amplitude is then given by

$$\begin{aligned}
 H & \begin{array}{c} j_k \\ \uparrow \\ c_1 \\ \uparrow \\ m_1 \\ \uparrow \\ j_i \quad j_j \\ \swarrow \quad \searrow \end{array} = \sum_{a,b,c_2} \tilde{H}_{a,b;c_2}^{j_i j_j; c_1}(j_k; m_1) \begin{array}{c} j_k \\ \uparrow \\ c_2 \\ \uparrow \\ m_1 \\ \uparrow \\ a \quad b \\ \swarrow \quad \searrow \\ j_i \quad j_j \end{array} \\
 & + \sum_{\substack{b,c_2 \\ a_1,a_2}} \tilde{(-)}^{2m_1} (-)^{j_i+j_j+c_1} \begin{Bmatrix} a_1 & j_j & j_k \\ c_1 & m_1 & j_i \end{Bmatrix} H_{b,c_2;a_2}^{j_j j_k; a_1}(j_i; m_1) \begin{array}{c} j_k \\ \uparrow \\ c_2 \\ \uparrow \\ m_1 \\ \uparrow \\ a_2 \\ \uparrow \\ b \\ \swarrow \quad \searrow \\ j_i \quad j_j \end{array} \\
 & + \sum_{\substack{c_2,a \\ b_1,b_2}} \tilde{(-)}^{2m_1} (-)^{j_i+b_1+j_k} \begin{Bmatrix} j_i & b_1 & j_k \\ m_1 & c_1 & j_j \end{Bmatrix} H_{c_2,a;b_2}^{j_k j_i; b_1}(j_j; m_1) \begin{array}{c} j_k \\ \uparrow \\ c_2 \\ \uparrow \\ m_1 \\ \uparrow \\ a \\ \uparrow \\ m_1 \\ \uparrow \\ b_2 \\ \swarrow \quad \searrow \\ j_i \quad j_j \end{array}
 \end{aligned} \tag{41}$$

where

$$H_{ab;y}^{ij;x}(k; m_1) = \epsilon(i, j, k) \frac{8i}{N_m^2 \kappa l_p^2} \sum_{\substack{z_1, m_2 \\ m_3 \in 2\mathbb{N}+1}} \sum_{z_2} \tilde{(-)}^{m_1+z_1+x+i+a+2j} \begin{Bmatrix} m & m_1 & m_2 \\ x & z_1 & k \end{Bmatrix} V_{z_2}^x(i, j|z_1; m_2) \begin{Bmatrix} m_2 & z_1 & z_2 \\ m_1 & k & y \\ m & m & m_3 \end{Bmatrix} \begin{Bmatrix} i & j & z_2 \\ a & b & y \\ m & m & m_3 \end{Bmatrix}.$$

and $H_{ab;y}^{ij;x} = H_{ba;y}^{ji;x}$.

This concludes the discussion of the action of the Euclidean constraint on trivalent vertices, invariant as well as variant ones. The matrix elements for higher valent nodes can be in principle obtained by analogous methods (see e.g. [27] for four-valent vertices).

V. MATRIX ELEMENTS OF \hat{T}

Having all the necessary tools at hand we can now proceed to calculate the matrix elements of

$$\hat{T} \propto \epsilon_{ijk} \text{Tr}_m [h_{s_i} [h_{s_i^{-1}}, \hat{K}] h_{s_j} [h_{s_j^{-1}}, \hat{K}] h_{s_k} [h_{s_k^{-1}}, \hat{V}]].$$

Because the volume and therefore also the extrinsic curvature $\hat{K} = \frac{i}{l_p^2 \gamma} [\hat{V}, \hat{H}]$ of a gauge-invariant trivalent node is zero, the only nonvanishing contribution of \hat{T} on such nodes is proportional to¹¹

$$\epsilon_{ijk} \text{Tr}_m [h_{s_i} \hat{K} h_{s_i^{-1}} h_{s_j} [h_{s_j^{-1}}, \hat{K}] h_{s_k} \hat{V} h_{s_k^{-1}}].$$

The only unknown part in this expression is the extrinsic curvature that will be discussed next before evaluating the full trace in Secs. VB and VC.

A. Extrinsic curvature of gauge-variant trivalent nodes

As the extrinsic curvature is linear in \hat{H} , its action on a trivalent (variant) vertex decomposes into a sum,

$$\hat{K} = \frac{i}{l_p^2 \gamma} (\hat{K}(\alpha_{ij}) + \hat{K}(\alpha_{jk}) + \hat{K}(\alpha_{ki})), \tag{42}$$

of the three contributions, $\hat{K}(\alpha_{ij}) := \frac{4i}{N_m^2 k l_p^2} [\hat{V}, \text{Tr}_m [(h_{\alpha_{ij}} - h_{\alpha_{ji}}) h_{s_k} V h_{s_k^{-1}}]]$, associated to the loops α_{ij} . By combining the results of Secs. IIIC and IVB one finds immediately

$$K_{ab;c_2}^{jij;c_1}(j_k; m_1) = \sum_{x,y} d_y H_{a b; y}^{ijj;x}(j_k; m_1) \left[\frac{1}{d_{c_2}} V_{c_2}^y(a, b, j_k; m_1) \delta_{x,c_1} - V_x^{c_1}(j_i, j_j | j_k; m_1) \delta_{y,c_2} \right],$$

for

$$\hat{K}(\alpha_{ij}) := \sum_{a,b,c_2} K_{a b; c_2}^{jij;c_1}(j_k; m_1) \tag{43}$$

and the full extrinsic curvature is given by

$$\hat{K} = \sum_{a_1} (-)^{2m_1} (-)^{j_i+j_j+c_1} \left\{ \begin{matrix} j_i & j_j & c_1 \\ j_k & m_1 & a_1 \end{matrix} \right\} \sum_{a_2,b,c_2} K_{bc_2;a_2}^{jjj;a_1}(j_i; m_1) + \sum_{b_1} (-)^{j_i+b_1+j_k+2m_1} \left\{ \begin{matrix} j_i & j_j & c_1 \\ m_1 & j_k & b_1 \end{matrix} \right\} \sum_{a,b,c_2} K_{c_2 a; b_2}^{jki;b_1}(j_j; m_1) + \sum_{a,b,c_2} K_{a b; c_2}^{jij;c_1}(j_k; m_1) \tag{44}$$

Note, due to the symmetries of volume and Euclidean constraint $K_{a b; c_2}^{jij;c_1} = (-)^{c_1-c_2} K_{b a; c_2}^{jij;c_1}$.

¹¹This is not true in general.

B. Matrix elements of $\text{Tr}_m[h_{s_i} \hat{K} h_{s_i^{-1}} h_{s_j} \hat{K} h_{s_j^{-1}} h_{s_k} V h_{s_k^{-1}}]$

The missing link to write down the complete action of \hat{T} on trivalent invariant nodes are the contributions $\text{Tr}_m[h_{s_i} \hat{K} h_{s_i^{-1}} h_{s_j} \hat{K} h_{s_j^{-1}} h_{s_k} V h_{s_k^{-1}}]$ and $\text{Tr}_m[h_{s_i} \hat{K} h_{s_i^{-1}} \hat{K} h_{s_k} V h_{s_k^{-1}}]$. The latter contribution is analyzed in the succeeding section while here the action of the first trace is evaluated. The term $h_{s_k} \hat{V} h_{s_k^{-1}}$ is just the same as for the Euclidean Hamiltonian. Therefore,

$$\begin{array}{c} j_k \\ | \\ \text{---} \\ | \\ \text{---} \\ / \quad \backslash \\ j_i \quad j_j \end{array} \xrightarrow{h_{s_j^{-1}} h_{s_k} \hat{V} h_{s_k^{-1}}} \sum_{c_1, b_1} \sum_{c_2} (-)^{2(j_k + j_j)} V_{c_2}^{j_k}(j_i, j_j | c_1; m) \begin{array}{c} j_k \\ | \\ \text{---} \\ | \\ \text{---} \\ / \quad \backslash \\ j_i \quad j_j \end{array} \quad (45)$$

Before acting with \hat{K} the dashed leg m must be erased from the diagram and \rightarrow moved to the appropriate place. This can be done simultaneously via Eqs. (26)–(28) so that \hat{K} acts on the above expression by

$$\begin{aligned}
 & \sum_{c_1, b_1} \sum_{c_2} V_{c_2}^{j_k}(j_i, j_j | c_1; m) \left[\sum_{\substack{a_1, b_2 \\ c_3, c_4}} (-)^{j_i - j_j - j_k} \begin{Bmatrix} c_1 & c_2 & m \\ c_3 & j_k & m \end{Bmatrix} \begin{Bmatrix} j_i & j_j & c_2 \\ m & c_3 & b_1 \end{Bmatrix} K_{a_1 b_2; c_4}^{j_i b_1; c_3}(j_k; m) \begin{array}{c} j_k \\ | \\ \text{---} \\ | \\ \text{---} \\ / \quad \backslash \\ j_i \quad j_j \end{array} \right. \\
 & + \sum_{\substack{a_1, a_2 \\ b_2, c_3}} (-)^{j_i + a_1 + c_1 + c_2} \begin{Bmatrix} c_1 & c_2 & m \\ j_i & a_1 & j_j \end{Bmatrix} \begin{Bmatrix} a_1 & j_j & c_1 \\ m & j_k & b_1 \end{Bmatrix} K_{b_2 c_3; a_2}^{b_1 j_k; a_1}(j_i; m) \begin{array}{c} j_k \\ | \\ \text{---} \\ | \\ \text{---} \\ / \quad \backslash \\ j_i \quad j_j \end{array} \\
 & \left. + \sum_{\substack{a_1, c_3 \\ b_2, b_3}} (-)^{j_j + b_2} \begin{Bmatrix} j_i & b_2 & j_k \\ j_j & b_1 & m \\ c_2 & m & c_1 \end{Bmatrix} K_{c_3 a_1; b_3}^{j_k j_i; b_2}(j_j; m) \begin{array}{c} j_k \\ | \\ \text{---} \\ | \\ \text{---} \\ / \quad \backslash \\ j_i \quad j_j \end{array} \right]
 \end{aligned}$$

In the next step $h_{s_i^{-1}} h_{s_i}$ is added. For the third term this is straightforward: h_{s_j} transforms b_1 into a dashed line and $h_{s_i^{-1}}$ can be coupled as usual via (21) resulting in

$$\sum \dots \sum_{a_2} \begin{array}{c} j_k \\ | \\ \text{---} \\ | \\ \text{---} \\ / \quad \backslash \\ j_i \quad j_j \end{array} \quad (46)$$

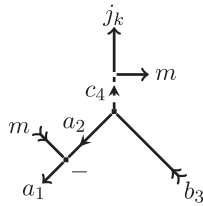
The most efficient way to proceed with the other two terms is to couple h_{s_j} via (17) and then use (25). This yields

$$\sum_{\tilde{a}_2, \tilde{b}_3} \dots \sum_{\tilde{a}_2, \tilde{b}_3} (-)^{2(a_1+b_2)} \text{Diagram} = \sum_{\tilde{a}_2, \tilde{b}_3} \dots \sum_{\tilde{a}_2, \tilde{b}_3} (-)^{j_j+c_4-a_1} \left\{ \begin{matrix} b_1 & b_2 & m \\ b_3 & j_j & m \end{matrix} \right\} \left\{ \begin{matrix} a_1 & b_2 & c_4 \\ b_3 & a_2 & m \end{matrix} \right\} \text{Diagram} \quad (47)$$

for the first term and

$$\sum_{\tilde{a}_3, \tilde{b}_3} \dots \sum_{\tilde{a}_3, \tilde{b}_3} (-)^{2(j_i+b_3)} \text{Diagram} = \sum_{\tilde{a}_3, \tilde{b}_3} \dots \sum_{\tilde{a}_3, \tilde{b}_3} (-)^{2(j_i+b_3)} (-)^{b_1+b_3} \left\{ \begin{matrix} b_1 & b_2 & m \\ b_3 & j_j & m \end{matrix} \right\} \text{Diagram} \quad (48)$$

for the second term. Since the newly created nodes are coplanar, \hat{V} as well as \hat{K} are vanishing on them no matter if they are gauge invariant or not. Therefore it suffices to calculate $\text{Tr}[h_{s_i} \hat{K} \dots]$ on the inner parts. Instead of considering the full diagram (47) it suffices to evaluate $\text{Tr}[h_{s_i} \hat{K} \dots]$ on



Inserting (44) and contracting with the last holonomy h_{s_i} results in

$$\sum_{\substack{\tilde{a}_3, \tilde{a}_4 \\ \tilde{b}_4, \tilde{c}_5}} (-)^{2a_4} K_{a_3 b_4; c_5}^{a_2 b_3; c_4}(j_k; m) \text{Diagram} + \sum_{\substack{\tilde{a}_3, \tilde{a}_4 \\ \tilde{b}_4, \tilde{c}_5}} (-)^{a_2+b_3+c_4+2m} \left\{ \begin{matrix} a_2 & b_3 & c_4 \\ j_k & m & a_3 \end{matrix} \right\} K_{b_4 c_5; a_4}^{b_3 c_4; a_3}(a_2; m) \text{Diagram} \\ + \sum_{\substack{\tilde{a}_3, \tilde{a}_4 \\ \tilde{b}_4, \tilde{b}_5, \tilde{c}_5}} (-)^{2(m+a_3)} (-)^{a_2+b_4+j_k} \left\{ \begin{matrix} a_2 & b_3 & c_4 \\ m & j_k & b_4 \end{matrix} \right\} K_{c_5 a_3; b_5}^{j_k a_2; b_4}(b_3; m) \text{Diagram}$$

for this node. Finally, all dashed parts of the graphics can be erased due to Eqs. (25) and (23). The other summands, (46) and (48), can be treated along the same lines. Except that in these cases the inner parts are of the same type as the node shown on the right-hand side of (45). Consequently, they have to be manipulated again to remove the dashed line m and move \rightarrow to the right place before acting with \hat{K} . The final result of this computation is

$$\begin{aligned}
 & \text{Tr}_m[h_{s_i} \hat{K} h_{s_i^{-1}} h_{s_j} \hat{K} h_{s_j^{-1}} h_{s_k} V h_{s_k^{-1}}] \begin{array}{c} j_k \\ \swarrow \quad \searrow \\ j_i \quad j_j \end{array} = \sum_{b_1, c_1}^{\sim} \sum_{c_2} V_{c_2}^{j_k}(j_i, j_j | c_1; m) \\
 & \left[\sum_{\substack{a_1, a_2, b_2 \\ b_3, c_3, c_4}}^{\sim} (-)^{j_i - a_1 + c_4 - j_k} \left\{ \begin{matrix} c_1 & c_2 & m \\ c_3 & j_k & m \end{matrix} \right\} \left\{ \begin{matrix} j_i & j_j & c_2 \\ m & c_3 & b_1 \end{matrix} \right\} K_{a_1 b_2; c_4}^{j_i b_1; c_3}(j_k; m) \left\{ \begin{matrix} b_1 & b_2 & m \\ b_3 & j_j & m \end{matrix} \right\} \left\{ \begin{matrix} a_1 & b_2 & c_4 \\ b_3 & a_2 & m \end{matrix} \right\} \right. \\
 & \left[\sum_{\substack{a_3, a_4 \\ b_4, c_5}}^{\sim} K_{a_3 b_4; c_5}^{a_2 b_3; c_4}(j_k; m) (-)^{a_2 + a_3 - a_4 + b_4 + c_5} \left\{ \begin{matrix} a_2 & a_3 & m \\ a_4 & a_1 & m \end{matrix} \right\} \left\{ \begin{matrix} a_3 & b_4 & c_5 \\ j_k & m & a_4 \end{matrix} \right\} \right. \\
 & \left. + \sum_{\substack{a_3, b_4 \\ c_5}}^{\sim} (-)^{b_3 + c_4 - a_2} \left\{ \begin{matrix} a_1 & a_3 & m \\ j_k & c_4 & b_3 \end{matrix} \right\} K_{b_4 c_5; a_1}^{b_3 j_k; a_3}(a_2; m) \right. \\
 & \left. + \sum_{\substack{a_3, a_4 \\ b_4, b_5, c_5}}^{\sim} (-)^{a_1 + a_2 - a_3 + a_4} (-)^{b_3 + b_4 + j_k + c_5} \left\{ \begin{matrix} b_3 & b_4 & m \\ j_k & c_4 & a_2 \end{matrix} \right\} K_{c_5 a_3; b_5}^{j_k a_2; b_4}(b_3; m) \left\{ \begin{matrix} a_2 & a_3 & m \\ a_4 & a_1 & m \end{matrix} \right\} \left\{ \begin{matrix} a_3 & b_5 & c_5 \\ b_3 & a_4 & m \end{matrix} \right\} \right] \\
 & + \sum_{\substack{a_1, a_2 \\ b_2, b_3, c_3}}^{\sim} (-)^{a_1 - j_i + b_1 - b_3 + c_1 + c_2} \left\{ \begin{matrix} c_1 & c_2 & m \\ j_i & a_1 & j_j \end{matrix} \right\} \left\{ \begin{matrix} a_1 & j_j & c_1 \\ m & j_k & b_1 \end{matrix} \right\} K_{b_2 c_3; a_2}^{b_1 j_k; a_1}(j_i; m) \left\{ \begin{matrix} b_1 & b_2 & m \\ b_3 & j_j & m \end{matrix} \right\} \\
 & \left[\sum_{\substack{a_3, a_4 \\ b_4, c_4, c_5}}^{\sim} (-)^{a_3 - a_4 + a_5 + b_4 + c_5} \left\{ \begin{matrix} a_2 & b_2 & c_3 \\ c_4 & m & j_i \end{matrix} \right\} \left\{ \begin{matrix} j_i & b_2 & c_4 \\ b_3 & a_2 & m \end{matrix} \right\} K_{a_4 b_4; c_4}^{a_3 b_3; c_3}(c_3; m) \left\{ \begin{matrix} a_3 & a_4 & m \\ a_5 & j_i & m \end{matrix} \right\} \left\{ \begin{matrix} a_4 & b_4 & c_5 \\ c_3 & m & a_5 \end{matrix} \right\} \right. \\
 & \left. + \sum_{\substack{a_3, a_4 \\ b_4, c_4}}^{\sim} (-)^{j_i - a_2 + a_4 + b_2 + c_3} \left\{ \begin{matrix} j_i & a_2 & m \\ a_4 & a_3 & m \end{matrix} \right\} \left\{ \begin{matrix} j_i & b_2 & c_4 \\ b_3 & a_4 & m \end{matrix} \right\} K_{b_4 c_4; a_1}^{b_3 c_3; a_4}(a_3; m) \right. \\
 & \left. + \sum_{\substack{a_3, a_4 \\ b_4, b_5, c_4}}^{\sim} (-)^{a_2 + a_4 - a_5 + b_2 + c_4} \left\{ \begin{matrix} b_2 & m & b_3 \\ c_3 & a_3 & b_4 \\ a_2 & j_i & m \end{matrix} \right\} K_{c_4 a_4; b_5}^{c_3 a_3; b_4}(b_3; m) \left\{ \begin{matrix} a_3 & a_4 & m \\ a_5 & j_i & m \end{matrix} \right\} \left\{ \begin{matrix} a_4 & b_5 & c_4 \\ b_3 & a_5 & m \end{matrix} \right\} \right]
 \end{aligned}$$

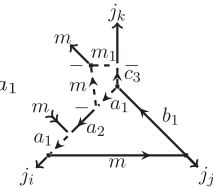
$$\begin{aligned}
 & + \sum_{\substack{a_1, a_2 \\ b_2, b_3, c_3}} (-)^{b_1 - b_2 + m} \begin{Bmatrix} j_i & b_2 & j_k \\ j_j & b_1 & m \\ c_2 & m & c_1 \end{Bmatrix} K_{c_3 a_1; b_3}^{j_k j_i; b_2}(b_1; m) \\
 & \left[\sum_{\substack{a_3, a_4 \\ b_4, c_4, c_5}} (-)^{a_2 - a_3 + a_4 + j_j + b_3 + b_4 + c_3 + c_4 + c_5 + m} \begin{Bmatrix} a_1 & b_3 & c_3 \\ m & c_4 & b_1 \end{Bmatrix} \begin{Bmatrix} a_1 & b_1 & c_4 \\ j_j & a_2 & m \end{Bmatrix} K_{a_3 b_4; c_5}^{a_2 j_j; c_4}(c_3; m) \begin{Bmatrix} a_2 & a_3 & m \\ a_4 & a_1 & m \end{Bmatrix} \begin{Bmatrix} a_3 & b_4 & c_4 \\ c_3 & m & a_4 \end{Bmatrix} \right. \\
 & \quad \left. + \sum_{a_3, c_4} (-)^{a_2 + b_3 - c_3 + m} \begin{Bmatrix} j_j & b_1 & m \\ c_3 & b_3 & a_1 \\ a_3 & m & a_2 \end{Bmatrix} K_{b_4 c_4; a_1}^{j_j c_3; a_3}(a_2; m) \right. \\
 & \quad \left. + \sum_{\substack{a_3, a_4 \\ b_4, b_5, c_4}} (-)^{a_4 - a_3 + j_j - b_1 + c_3 + c_4 + m} \begin{Bmatrix} b_1 & b_3 & m \\ b_4 & j_j & m \end{Bmatrix} \begin{Bmatrix} a_1 & b_3 & c_3 \\ b_4 & a_2 & m \end{Bmatrix} K_{c_4 a_3; b_5}^{c_3 a_2; b_4}(j_j; m) \begin{Bmatrix} a_2 & a_3 & m \\ a_4 & a_1 & m \end{Bmatrix} \begin{Bmatrix} a_3 & b_5 & c_4 \\ j_j & a_4 & m \end{Bmatrix} \right]
 \end{aligned}$$

C. Computation of $\text{Tr}_m[h_{s_i} \hat{K} h_{s_i}^{-1} \hat{K} h_{s_k} V h_{s_k}^{-1}]$

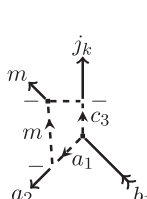
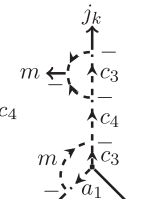
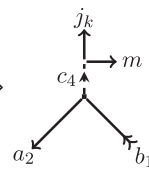
As before $h_{s_k} \hat{V} h_{s_k}^{-1}$ produces a double noninvariant node transforming in the representation $\mathcal{H}_m^* \otimes \mathcal{H}_m$ where * denotes the adjoint. In contrast to the above, the extrinsic curvature \hat{K} is directly acting on this node. Therefore, it is advisable to introduce an artificial coupling as was done for the volume:

$$\begin{aligned}
 & \begin{array}{c} j_k \\ \diagup \quad \diagdown \\ j_i \quad j_j \end{array} \xrightarrow{h_{s_k} \hat{V} h_{s_k}^{-1}} \sum_{c_1, c_2} d_{c_1} (-)^{2j_k} V_{c_2}^{j_k}(j_i, j_j | c_1; m) \begin{array}{c} j_k \\ \leftarrow m \\ \leftarrow c_2 \\ \leftarrow m \\ \uparrow c_1 \\ \diagup \quad \diagdown \\ j_i \quad j_j \end{array} \\
 & = \sum_{c_1, m_1} \sum_{c_2} V_{c_2}^{j_k}(j_i, j_j | c_1; m) (-)^{c_1 + c_2 + m} \begin{Bmatrix} m & m & m_1 \\ j_k & c_2 & c_1 \end{Bmatrix} \begin{array}{c} j_k \\ \leftarrow m_1 \\ \leftarrow m \\ \leftarrow m \\ \uparrow c_1 \\ \diagup \quad \diagdown \\ j_i \quad j_j \end{array}
 \end{aligned}$$

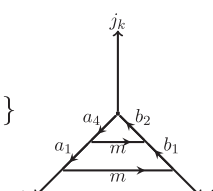

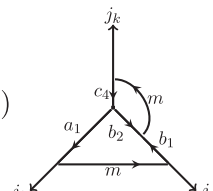
Recall that m and m_1 are purely internal so that the curvature operator only registers a trivalent node transforming in spin m_1 and the previous results (44) can be employed. Thus $h_{s_i}^{-1} \hat{K}$ transforms the above expression into

$$\sum_{c_1, m_1} \sum_{c_2} V_{c_2}^{j_k}(j_i, j_j | c_1; m) (-)^{c_1+c_2+m} \left\{ \begin{matrix} m & m & m_1 \\ j_k & c_2 & c_1 \end{matrix} \right\} \left[\sum_{\substack{a_1, a_2 \\ b_1, c_3}} \tilde{K}_{a_1 b_1; c_3}^{j_i j_j; c_2}(j_k; m_1) (-)^{2a_1} \right.

 $\left. + \dots \right]$$$

The link m_1 can be decoupled and parts of the internal lines can be removed:

$$= \sum_{c_3} (-)^{2c_4}

 $= \sum_{c_3} (-)^{2c_4}

 $= \sum_{c_4} (-)^{2c_4} (-)^{b_1+j_k-a_1} \left\{ \begin{matrix} a_1 & b_1 & c_3 \\ c_4 & m & a_2 \end{matrix} \right\} \left\{ \begin{matrix} m & m & m_1 \\ j_k & c_3 & c_4 \end{matrix} \right\}
$$$$

The rest of the calculation is completely equivalent to the one in the previous section. With all other terms one can proceed similarly, resulting in

$$\sum_{c_1, m_1} \sum_{c_2} V_{c_2}^{j_k}(j_i, j_j | c_1; m) (-)^{c_1+c_2+m} \left\{ \begin{matrix} m & m & m_1 \\ j_k & c_2 & c_1 \end{matrix} \right\} \left[\sum_{\substack{a_1, a_2 \\ b_1, c_3}} \tilde{K}_{a_1 b_1; c_3}^{j_i j_j; c_2}(j_k; m_1) \right.

 $\left. \left[\sum_{\substack{a_3, a_4 \\ b_2, c_4, c_5}} (-)^{a_3+a_4+m} (-)^{b_2-b_1+j_k+c_5+m_1} \left\{ \begin{matrix} a_1 & b_1 & c_3 \\ c_4 & m & a_2 \end{matrix} \right\} \left\{ \begin{matrix} j_k & c_3 & m_1 \\ m & m & c_4 \end{matrix} \right\} K_{a_3 b_2; c_5}^{a_2 b_1; c_4}(j_k; m) \left\{ \begin{matrix} a_2 & a_3 & m \\ a_4 & a_1 & m \end{matrix} \right\} \left\{ \begin{matrix} a_3 & b_2 & c_5 \\ j_k & m & a_4 \end{matrix} \right\} \right. \right.

 $+ \sum_{\substack{a_3, b_2 \\ c_4}} (-)^{a_1+a_2+a_3+b_1+c_3+m} \left\{ \begin{matrix} a_1 & m_1 & a_3 \\ m & a_2 & m \end{matrix} \right\} \left\{ \begin{matrix} a_1 & m_1 & a_3 \\ j_k & b_1 & c_3 \end{matrix} \right\} K_{b_2 c_4; a_1}^{b_1 j_k; a_3}(a_2; m) \left. \right.

 $+ \sum_{\substack{a_3, a_4 \\ b_2, b_3, c_4}} (-)^{a_2+a_3+a_4+b_1-j_k+c_3+c_4+m} \left\{ \begin{matrix} a_1 & b_1 & c_3 \\ a_2 & b_2 & j_k \\ m & m & m_1 \end{matrix} \right\} K_{c_4 a_3; b_3}^{j_k a_2; b_2}(b_1; m) \left\{ \begin{matrix} a_2 & a_3 & m \\ a_4 & a_1 & m \end{matrix} \right\} \left\{ \begin{matrix} a_3 & b_2 & c_5 \\ j_k & m & a_4 \end{matrix} \right\} \left. \right]$$$$$

$$\text{Tr}[h_{s_j} \hat{K} h_{s_j^{-1}} h_{s_i} \hat{K} h_{s_i^{-1}} h_{s_k} \hat{V} h_{s_k^{-1}}] \begin{array}{c} j_k \\ \swarrow \quad \searrow \\ j_i \quad j_j \end{array} = (-)^{j_i+j_j+j_k} \text{Tr}[h_{s_j} \hat{K} h_{s_j^{-1}} h_{s_i} \hat{K} h_{s_i^{-1}} h_{s_k} \hat{V} h_{s_k^{-1}}] \begin{array}{c} j_k \\ \swarrow \quad \searrow \\ j_j \quad j_i \end{array}$$

The trace can now be evaluated as above treating i as j and j as i . Finally the edges should be flipped back:

$$\begin{aligned} \text{Tr}[h_{s_j} \hat{K} h_{s_j^{-1}} h_{s_i} \hat{K} h_{s_i^{-1}} h_{s_k} \hat{V} h_{s_k^{-1}}] \begin{array}{c} j_k \\ \swarrow \quad \searrow \\ j_i \quad j_j \end{array} &= (-)^{j_i+j_j+j_k} \sum_{a_1, c_1} \sum_{c_2} (-)^{j_k-c_2} V_{c_2}^{j_k}(j_i, j_j | c_1; m) \\ &\left[\sum_{\substack{b_1, b_2, a_2 \\ a_3, c_3, c_4}} (-)^{j_j-b_1+c_4-j_k} \left\{ \begin{matrix} c_1 & c_2 & m \\ c_3 & j_k & m \end{matrix} \right\} \left\{ \begin{matrix} j_j & j_i & c_2 \\ m & c_3 & a_1 \end{matrix} \right\} (-)^{c_3-c_4} K_{a_2 b_1; c_4}^{-a_1 j_j; c_3}(j_k; m) \left\{ \begin{matrix} a_1 & a_2 & m \\ a_3 & j_i & m \end{matrix} \right\} \left\{ \begin{matrix} b_1 & a_2 & c_4 \\ a_3 & b_2 & m \end{matrix} \right\} \right. \\ &\left. \left[\sum_{\substack{b_3, b_4 \\ a_4, c_5}} (-)^{c_4-c_5} K_{a_4 b_3; c_5}^{-a_3 b_2; c_4}(j_k; m) (-)^{b_2+b_3-b_4+a_4+c_5} \left\{ \begin{matrix} b_2 & b_3 & m \\ b_4 & b_1 & m \end{matrix} \right\} \left\{ \begin{matrix} b_3 & a_4 & c_5 \\ j_k & m & b_4 \end{matrix} \right\} (-)^{j_k+j_j+j_i} \right. \right. \\ &\left. \left. \begin{array}{c} j_k \\ \swarrow \quad \searrow \\ j_i \quad j_j \end{array} \begin{array}{c} a_4 \quad b_4 \\ \swarrow \quad \searrow \\ a_1 \quad m \quad b_3 \end{array} + \dots \right] + \dots \right] \end{aligned}$$

where we used $V_{c_2}^{j_k}(j_i, j_j | c_1; m) = (-)^{j_k-c_2} V_{c_2}^{j_k}(j_j, j_i | c_1; m)$, $K_{a_2 b_1; c_4}^{-a_1 j_j; c_3} = (-)^{c_3-c_4}$, and

$$\begin{array}{c} j_k \\ \swarrow \quad \searrow \\ j_i \quad j_j \end{array} \begin{array}{c} b_4 \quad a_4 \\ \swarrow \quad \searrow \\ b_1 \quad m \quad a_3 \end{array} = \underbrace{(-)^{j_k+a_4+b_4} (-)^{b_4+b_1+m} (-)^{j_j+b_1+m} (-)^{a_4+a_3+m} (-)^{j_i+a_3+m}}_{(-)^{j_k+j_j+j_i}} \begin{array}{c} j_k \\ \swarrow \quad \searrow \\ j_i \quad j_j \end{array} \begin{array}{c} a_4 \quad b_4 \\ \swarrow \quad \searrow \\ a_1 \quad m \quad b_3 \end{array}$$

Note, that here the sign generated by the first switch of the edges is canceled by the one originating from restoring the old orientations. This is a generic property and applies to *all* terms of the full expression. Only signs arising from volume and extrinsic curvature remain. The matrix elements corresponding to cyclic permutations of (i, j, k) are simply obtained by exchanging the labels $(j_i, a.)$ by $(j_j, b.)$, $(j_j, b.)$ by $(j_k, c.)$, and so forth.

The second contribution $\text{Tr}[h_{s_i} \hat{K} h_{s_i^{-1}} \hat{K} h_{s_k} \hat{V} h_{s_k^{-1}}]$ can be treated along the same lines. The value of $\text{Tr}[h_{s_j} \hat{K} h_{s_j^{-1}} \hat{K} h_{s_k} \hat{V} h_{s_k^{-1}}]$ can be calculated by first flipping the edges so that i can be treated as j and vice versa and afterwards restoring the original orientation.

VI. CONCLUSION AND OUTLOOK

In this article we derived for the first time an explicit formula for the matrix elements of the full Hamiltonian constraint in LQG including the Lorentzian part. As we

already pointed out, this constraint plays a major role in any canonical quantization program for GR based on real Ashtekar-Barbero variables so that the methods developed in the course of the calculation are also of interest in these approaches, e.g. the master constraint approach. On the other hand, the tools developed to compute the action of the curvature [especially the loop trick (36)] or extrinsic curvature can be easily adapted to models with nongraph-changing operators, as the extended master constraint ansatz or AQG, by extending the loops involved in the regularization in such a way that no new links are created.

By exploiting several new recoupling identities, we significantly simplified the matrix element so that the recoupling part is totally captured in $6j$ and $9j$ symbols for which symmetry properties and explicit formulas are well known. The final expression still depends on the volume but can be easily implemented on a computer for further investigations. We also expect to get interesting

insight from a large j expansion or the application in symmetry reduced models. Of special interest would be, for example, the recently introduced model [41,42] that keeps the original SU(2) structure of the theory but has a diagonal volume operator so that it may be possible to give an analytical closed formula for the whole constraint within this Ansatz. Finally the presented analysis opens the way for a comparison with the covariant approach, because the spin-foam vertex amplitudes are expected to be annihilated by the Hamiltonian constraint [27]. As the matching between the canonical and covariant kinematics [43] led to the upgrade of the old Barret-Crane model [44] to the new EPRL-model [45], the matching with the dynamical constraint is expected to shed new light onto the canonical-covariant joint theory.

ACKNOWLEDGMENTS

The authors wish to thank T. Thiemann for useful discussions and L. Cottrell for a careful reading of the manuscript. The work of E. A. was partially supported by the grant of Polish Narodowe Centrum Nauki nr DEC-2011/02/A/ST2/00300. A.Z. acknowledges financial support of the ‘‘Elitenetzwerk Bayern’’ on the grounds of ‘‘Bayerische Eliteforder Gesetz.’’

APPENDIX A: MORE ON 3j’S, 6j’S, AND 9j’S

For self-containedness some important properties of nj symbols are listed here. Introductions to recoupling theory can be found in various textbooks on quantum mechanics and quantum angular momentum, e.g. [40]. For an extensive list of properties of nj symbols, see e.g. [46]

3j-Symbols

Relation to Clebsh-Gordan coefficients:

$$\langle a, \alpha; b, \beta | c, \gamma \rangle = (-)^{b-a+\gamma} \sqrt{2c+1} \begin{pmatrix} a & b & c \\ \alpha & \beta & -\gamma \end{pmatrix}$$

where $|b, \beta; a, \alpha\rangle = |b, \beta\rangle \otimes |a, \alpha\rangle$

Compatibility criteria

If one (or several) of the following rules is violated, then

$$\begin{pmatrix} a & b & c \\ \alpha & \beta & \gamma \end{pmatrix}$$

is vanishing:

(i) $a, b, c \in \frac{1}{2}\mathbb{N}, a \pm \alpha \in \mathbb{N}, -a \leq \alpha \leq a, \dots$

(ii) $\alpha + \beta + \gamma = 0$

(iii) $a + b + c \in \mathbb{N}, |a - b| \leq c \leq a + b$ (triangle inequality)

Symmetries

$$\begin{pmatrix} a & b & c \\ \alpha & \beta & \gamma \end{pmatrix} = (-)^{a+b+c} \begin{pmatrix} a & b & c \\ -\alpha & -\beta & -\gamma \end{pmatrix} = (-)^{a+b+c} \begin{pmatrix} b & a & c \\ \beta & \alpha & \gamma \end{pmatrix} = \begin{pmatrix} b & c & a \\ \beta & \gamma & \alpha \end{pmatrix}$$

6j symbols

Definition in terms of 3j’s

$$\begin{Bmatrix} j_1 & j_2 & j_3 \\ j_4 & j_5 & j_6 \end{Bmatrix} = \sum_{\mu_1, \dots, \mu_6} (-)^{\sum_{i=1}^6 (j_i - \mu_i)} \begin{pmatrix} j_1 & j_2 & j_3 \\ \mu_1 & \mu_2 & -\mu_3 \end{pmatrix} \begin{pmatrix} j_1 & j_5 & j_6 \\ -\mu_1 & \mu_5 & \mu_6 \end{pmatrix} \\ \times \begin{pmatrix} j_4 & j_5 & j_3 \\ \mu_4 & -\mu_5 & \mu_3 \end{pmatrix} \begin{pmatrix} j_4 & j_2 & j_6 \\ -\mu_4 & -\mu_2 & -\mu_6 \end{pmatrix}$$

Symmetries

$$\begin{Bmatrix} a & b & c \\ d & e & f \end{Bmatrix} = \begin{Bmatrix} b & a & c \\ e & d & f \end{Bmatrix} = \begin{Bmatrix} b & c & a \\ e & f & d \end{Bmatrix} = \begin{Bmatrix} d & e & c \\ a & b & f \end{Bmatrix} = \begin{Bmatrix} d & b & f \\ a & e & c \end{Bmatrix} = \begin{Bmatrix} a & e & f \\ d & b & c \end{Bmatrix}$$

Compatibility

$$\begin{Bmatrix} a & b & c \\ d & e & f \end{Bmatrix} = 0$$

unless the triangle inequalities hold for $\{a, b, c\}$, $\{a, e, f\}$, $\{d, b, f\}$, and $\{d, e, c\}$

Orthogonality

$$\sum_x d_x \begin{Bmatrix} a & b & x \\ d & e & c \end{Bmatrix} \begin{Bmatrix} a & b & x \\ d & e & c' \end{Bmatrix} = \delta_{c,c'} \frac{1}{d_c}$$

if the compatibility requirements are fulfilled, with $d_x = 2x + 1$, $d_c = 2c + 1$ the dimensions of the representations.

9j symbols

Definition by 3j's

$$\begin{Bmatrix} j_1 & j_2 & j_3 \\ j_4 & j_5 & j_6 \\ j_7 & j_8 & j_9 \end{Bmatrix} = \sum_{\mu_1, \dots, \mu_9} (-1)^{\sum_i (j_i - \mu_i)} \begin{pmatrix} j_1 & j_2 & j_3 \\ \mu_1 & \mu_2 & \mu_3 \end{pmatrix} \begin{pmatrix} j_4 & j_5 & j_6 \\ \mu_4 & \mu_5 & \mu_6 \end{pmatrix} \begin{pmatrix} j_7 & j_8 & j_9 \\ \mu_7 & \mu_8 & \mu_9 \end{pmatrix} \\ \times \begin{pmatrix} j_1 & j_4 & j_7 \\ -\mu_1 & -\mu_4 & -\mu_7 \end{pmatrix} \begin{pmatrix} j_2 & j_6 & j_8 \\ -\mu_2 & -\mu_6 & -\mu_8 \end{pmatrix} \begin{pmatrix} j_3 & j_6 & j_9 \\ -\mu_3 & -\mu_6 & -\mu_9 \end{pmatrix}$$

Definition by 6j's

$$\begin{Bmatrix} a & f & r \\ d & q & e \\ p & c & b \end{Bmatrix} := \sum_x d_x (-1)^{2x} \begin{Bmatrix} a & b & x \\ c & d & p \end{Bmatrix} \begin{Bmatrix} c & d & x \\ e & f & q \end{Bmatrix} \begin{Bmatrix} e & f & x \\ a & b & r \end{Bmatrix}$$

Symmetries

$$\begin{Bmatrix} a & f & r \\ d & q & e \\ p & c & b \end{Bmatrix} = (-1)^S \begin{Bmatrix} d & q & e \\ a & f & r \\ p & c & b \end{Bmatrix} = (-1)^S \begin{Bmatrix} a & f & r \\ p & c & b \\ d & q & e \end{Bmatrix} \\ = (-1)^S \begin{Bmatrix} f & a & r \\ q & d & e \\ c & p & b \end{Bmatrix} = (-1)^S \begin{Bmatrix} a & r & f \\ d & e & q \\ p & b & c \end{Bmatrix}$$

where $S = a + b + c + d + e + f + p + q + r$.

APPENDIX B: VOLUME

For the sake of completeness the volume operator is briefly reviewed and the graphical framework for computing the action is discussed here, closely following [29,32]. Thereby we restrict our attention to the Ashtekar-Lewandowski volume [31], which was also analyzed in greater detail in [34].

1. General properties

Let T_s be a cylindrical function on a spin network s and let $\mathcal{V}(\Gamma)$ denote the set of nodes of the underlying graph Γ . The volume operator \hat{V} acts on T_s by

$$\hat{V} T_s = \sum_{v \in \mathcal{V}(\Gamma)} \hat{V}_v T_s, \quad (\text{B1})$$

where

$$\hat{V}_v = l_p^3 \sqrt{\left| \frac{i}{16 \cdot 3!} \sum_{e_I \cap e_J \cap e_K = v} \epsilon(e_I, e_J, e_K) W_{[JK]} \right|}. \quad (\text{B2})$$

The sum extends over all triples (e_I, e_J, e_K) of edges adjacent to the vertex v , l_p denotes the Planck length, and $\epsilon(e_I, e_J, e_K)$ is determined by the orientation of the tangents \dot{e}_I at v , i.e. $\epsilon(e_I, e_J, e_K) = \text{sgn}[\det(\dot{e}_I, \dot{e}_J, \dot{e}_K)]$. The grasping operator

$$W_{[JK]} := \epsilon_{ijk} X_I^i X_J^j X_K^k \quad (\text{B3})$$

depends on the right invariant vector fields (of SU(2))

$$X_l^i := -i \text{Tr} \left[(h_{e_l} \sigma^i)^T \frac{\partial}{\partial h_{e_l}} \right] \quad (\text{B4})$$

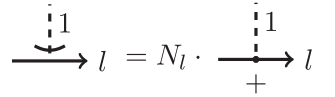
along the edge e_l at v . Here, e_l was chosen to be outgoing from v , σ^i are the Pauli matrices, and T denotes the transpose. The matrix elements $[\sigma^i]_B^A$ with spinorial indices $A, B = 0, 1$ and vector indices $i = 1, 2, 3$ are natural intertwiners of spin and vector representation [i.e. (1, 1/2, 1/2)]. Thus, X_l^i inserts an intertwiner $[\sigma^i]_B^A$ at an edge labeled by the fundamental representation. Since an irrep l is the completely symmetrized tensor product of $2l$ fundamental representations this can be immediately generalized to edges labeled by l . Similarly ϵ is a vector invariant intertwiner (1, 1, 1). Following the spirit of the graphical calculus, $W_{[JK]}$ can be visualized by



$$\sqrt{3!} \quad (\text{B5})$$

where each handle grasps an edge e at v . Note, this grasping depends on the orientation of e . Yet, we want to use $3j$ symbols rather than the invariants σ and ϵ . These differ from the corresponding $3j$'s by a normalization constant. The $3j$'s are normalized to one while $\text{Tr}[\epsilon^2] = 3!$ and $\sum_i \text{Tr}_l[(\sigma^i)^2] = 4[l(l+1)(2l+1)]$ where Tr_l indicates that the trace is evaluated in spin l . Thus, $\sqrt{3!}$ in (B5) stems from the normalization of ϵ . Each grasp of an edge colored by l

gives additionally a factor $N_l := -i2\sqrt{l(l+1)(2l+1)}$, in particular,



$$\quad (\text{B6})$$

When using this formalism,¹² one should keep in mind that the right invariant vector fields are derivative operators and hence only act on *true* holonomies. On the other hand W cannot change the graph itself but only alter the intertwiners. Consequently, the links in (B5) are only added at the vertex (in a dashed environment) and can be erased again by pure recoupling theory.

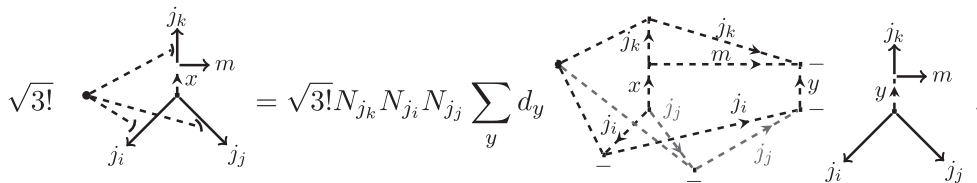
2. Trivalent nodes

The computational effort to determine the matrix elements of the volume operator is increasingly heavy as the valency of the nodes grows. Therefore we only discuss the case of a trivalent node



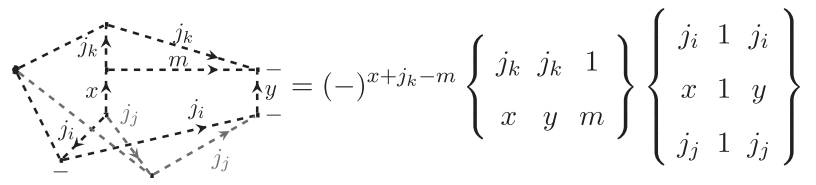
$$|v_x\rangle := \quad (\text{B7})$$

transforming in spin m . On a trivalent node \hat{V}_v reduces to $\frac{\beta}{4} \sqrt{|iW_{ijk}|}$ and the grasping yields



$$\quad (\text{B8})$$

In the second step a resolution of the identity in the intertwiner space was inserted (see Sec. III B). A careful evaluation by the usual methods reveals that



$$\quad (\text{B9})$$

The $6j$ in this equation is only nonzero if $(x, y, 1)$ obey the triangle inequality, i.e. if $|x - y| \leq 1$. But for $x = y$ the $9j$ symbol is vanishing since it is antisymmetric when switching the first and last columns. On the other hand, the $6j$ and the $9j$ are symmetric under the exchange of x and y for $y = x \pm 1$. Thus, if we work with rescaled nodes $|v_x\rangle_N = \sqrt{d_x} |v_x\rangle$, then

¹²This was developed first in [32]. However, they used another calculus based on Temperley-Lieb algebras which yields different normalizations.

$$\hat{W}_{[JK]}|v_x\rangle_N = \sum_y \tilde{W}_y^x |v_y\rangle_N$$

yields an antisymmetric matrix \tilde{W} , which has only subdiagonal and superdiagonal nonzero entries:

$$\tilde{W}_y^x = \delta_{y,x\pm 1} \sqrt{3!} \sqrt{d_x d_y} N_{j_k} N_{j_i} N_{j_j} (-)^{x+j_k-m} \begin{Bmatrix} j_k & j_k & 1 \\ x & y & m \end{Bmatrix} \begin{Bmatrix} j_i & 1 & j_i \\ x & 1 & y \\ j_j & 1 & j_j \end{Bmatrix}. \quad (\text{B10})$$

Fortunately, this matrix is diagonalizable so that the square root of W has a well-defined meaning. Suppose U is the (unitary) map that maps $\{|v_x\rangle_N\}$ to the eigenbasis of \tilde{W} , then the matrix elements of the volume [compare with (32)] are finally given by

$$V_y^x(j_i, j_j, j_k; m) = \frac{l_p^3}{4} \sqrt{\frac{d_y}{d_x}} [U^{-1}]_w^x \sqrt{|i[\tilde{W}_D]_w^z|} U_y^z \Lambda \quad (\text{B11})$$

where $\tilde{W}_D = U\tilde{W}U^{-1}$ is the diagonalized matrix. For small m the intertwiner space is low dimensional and this diagonalization does not cause problems:

- $m = 0$: For $m = 0$ the intertwiner space is one dimensional and therefore V annihilates gauge-invariant trivalent nodes.
- $m = \frac{1}{2}$: Here, the intertwiner space is two-dimensional and it is not hard to check that V is diagonal with matrix elements

$$V_y^x\left(j_i, j_j, j_k \middle| \frac{1}{2}\right) = \delta_y^x \frac{l_p^3}{4} \left[\left| i\sqrt{3!} \sqrt{d_{j_k+\frac{1}{2}} d_{j_k-\frac{1}{2}}} N_{j_k} N_{j_i} N_{j_j} \begin{Bmatrix} j_k & j_k & 1 \\ j_k+\frac{1}{2} & j_k-\frac{1}{2} & \frac{1}{2} \end{Bmatrix} \right. \right. \\ \left. \left. \times \begin{Bmatrix} j_i & 1 & j_i \\ j_k+\frac{1}{2} & 1 & j_k-\frac{1}{2} \\ j_j & 1 & j_j \end{Bmatrix} \right| \right]^{-\frac{1}{2}}.$$

- $m = 1$: For $m = 1$ \tilde{W} is a 3×3 matrix but does not have full rank. Nevertheless, it is diagonalizable when applying first a similarity transformation S (see [34]):

$$\tilde{W} = \begin{pmatrix} 0 & w_1 & 0 \\ -w_1 & 0 & w_2 \\ 0 & -w_2 & 0 \end{pmatrix} \xrightarrow{S} \begin{pmatrix} 0 & \frac{1}{w_1} \lambda^2 & 0 \\ -w_1 & 0 & 0 \\ 0 & -\frac{w_2}{w_1} & 0 \end{pmatrix} \xrightarrow{U} \lambda \begin{pmatrix} -i & 0 & 0 \\ 0 & i & 0 \\ 0 & 0 & 0 \end{pmatrix} \\ \rightarrow V = \frac{l_p^3}{4} \begin{pmatrix} \frac{|w_1|^2}{\lambda} & 0 & -\frac{|w_1 w_2|^2}{\lambda} \sqrt{\frac{2j_k+3}{2j_k-1}} \\ 0 & \lambda & 0 \\ \frac{|w_1 w_2|^2}{\lambda} \sqrt{\frac{2j_k-1}{2j_k+3}} & \frac{|w_2|}{|w_1|} & \frac{|w_2|^2}{\lambda} \end{pmatrix}$$

where

$$w_1 = (-)^{2(j_k-1)} \sqrt{3!} \sqrt{d_{j_k-1} d_{j_k}} N_{j_k} N_{j_i} N_{j_j} \left\{ \begin{matrix} j_k & j_k & 1 \\ j_k-1 & j_k & \frac{1}{2} \end{matrix} \right\} \left\{ \begin{matrix} j_i & 1 & j_i \\ j_k-1 & 1 & j_k \\ j_j & 1 & j_j \end{matrix} \right\}$$

$$w_2 = (-)^{2j_k-1} \sqrt{3!} \sqrt{d_{j_k+1} d_{j_k}} N_{j_k} N_{j_i} N_{j_j} \left\{ \begin{matrix} j_k & j_k & 1 \\ j_k+1 & j_k & \frac{1}{2} \end{matrix} \right\} \left\{ \begin{matrix} j_i & 1 & j_i \\ j_k+1 & 1 & j_k \\ j_j & 1 & j_j \end{matrix} \right\}$$

and $\lambda^2 = |w_1|^2 + |w_2|^2$.

-
- [1] A. Ashtekar, *Phys. Rev. Lett.* **57**, 2244 (1986).
 [2] J.F. Barbero, *Phys. Rev. D* **51**, 5507 (1995).
 [3] A. Ashtekar and J. Lewandowski, *Classical Quantum Gravity* **21**, R53 (2004).
 [4] T. Thiemann, *Modern Canonical Quantum General Relativity* (Cambridge University Press, Cambridge, England, 2007).
 [5] C. Rovelli, *Quantum Gravity* (Cambridge University Press, Cambridge, England, 2004).
 [6] P. Dirac, *Lectures on Quantum Mechanics* (Belfer Graduate School of Science, Yeshiva University Press, New York, 1964).
 [7] C. Rovelli and L. Smolin, *Phys. Rev. D* **52**, 5743 (1995).
 [8] R. Penrose, in *Quantum Theory and Beyond*, edited by T. Bastin (Cambridge University Press, New York, 1971).
 [9] A. Ashtekar, J. Lewandowski, D. Marolf, J. Mourao, and T. Thiemann, *J. Math. Phys. (N.Y.)* **36**, 6456 (1995).
 [10] T. Thiemann, *Phys. Lett. B* **380**, 257 (1996).
 [11] C. Rovelli, *Classical Quantum Gravity* **8**, 1613 (1991); V. Husain, *Nucl. Phys.* **B313**, 711 (1989); B. Bruegmann and J. Pullin, *Nucl. Phys.* **B363**, 221 (1991); R. Gambini, *Phys. Lett. B* **255**, 180 (1991); B. Bruegmann, R. Gambini, and J. Pullin, *Nucl. Phys.* **B385**, 587 (1992); C. Rovelli and L. Smolin, *Phys. Rev. Lett.* **72**, 446 (1994).
 [12] T. Thiemann, *Classical Quantum Gravity* **15**, 839 (1998).
 [13] T. Thiemann, *Classical Quantum Gravity* **15**, 875 (1998).
 [14] R. Gambini, J. Lewandowski, D. Marolf, and J. Pullin, *Int. J. Mod. Phys. D* **07**, 97 (1998); J. Lewandowski and D. Marolf, *Int. J. Mod. Phys. D* **07**, 299 (1998); L. Smolin, [arXiv:gr-qc/9609034](https://arxiv.org/abs/gr-qc/9609034).
 [15] T. Thiemann, *Classical Quantum Gravity* **23**, 2211 (2006); B. Dittrich and T. Thiemann, *Classical Quantum Gravity* **23**, 1025 (2006); T. Thiemann, *Classical Quantum Gravity* **23**, 2249 (2006).
 [16] K. Giesel and T. Thiemann, *Classical Quantum Gravity* **24**, 2465 (2007); **24**, 2499 (2007); **24**, 2565 (2007); **27**, 175009 (2010).
 [17] M. Domagala, K. Giesel, W. Kaminski, and J. Lewandowski, *Phys. Rev. D* **82**, 104038 (2010).
 [18] K. Giesel and T. Thiemann, [arXiv:1206.3807](https://arxiv.org/abs/1206.3807).
 [19] V. Husain and T. Pawłowski, *Phys. Rev. Lett.* **108**, 141301 (2012).
 [20] A. Ashtekar and P. Singh, *Classical Quantum Gravity* **28**, 213001 (2011).
 [21] M. Bojowald, *Living Rev. Relativity* **11**, 4 (2008).
 [22] A. Perez, *Living Rev. Relativity* **16**, 3 (2013); *Classical Quantum Gravity* **20**, R43 (2003); J. Baez, *Lect. Notes Phys.* **543**, 25 (2000); C. Rovelli, Proc. Sci., QGQGS2011 (2011) 003.
 [23] M.P. Reisenberger and C. Rovelli, *Phys. Rev. D* **56**, 3490 (1997).
 [24] K. Noui and A. Perez, *Classical Quantum Gravity* **22**, 1739 (2005); E. Alesci, K. Noui, and F. Sardelli, *Phys. Rev. D* **78**, 104009 (2008); B. Bahr, *Classical Quantum Gravity* **28**, 045002 (2011).
 [25] E. Alesci, *J. Phys. Conf. Ser.* **360**, 012041 (2012).
 [26] E. Alesci and C. Rovelli, *Phys. Rev. D* **82**, 044007 (2010).
 [27] E. Alesci, T. Thiemann, and A. Zipfel, *Phys. Rev. D* **86**, 024017 (2012).
 [28] R. Borissov, R. De Pietri, and C. Rovelli, *Classical Quantum Gravity* **14**, 2793 (1997).
 [29] M. Gaul and C. Rovelli, *Classical Quantum Gravity* **18**, 1593 (2001).
 [30] C. Rovelli and L. Smolin, *Nucl. Phys.* **B442**, 593 (1995); **B456**, 753(E) (1995).
 [31] A. Ashtekar and J. Lewandowski, *Adv. Theor. Math. Phys.* **1**, 388 (1998); J. Lewandowski, *Classical Quantum Gravity* **14**, 71 (1997).
 [32] R. De Pietri and C. Rovelli, *Phys. Rev. D* **54**, 2664 (1996).
 [33] T. Thiemann, *J. Math. Phys. (N.Y.)* **39**, 3347 (1998).
 [34] J. Brunnemann and T. Thiemann, *Classical Quantum Gravity* **23**, 1289 (2006).
 [35] E. Bianchi, P. Dona, and S. Speziale, *Phys. Rev. D* **83**, 044035 (2011).
 [36] J. Brunnemann and D. Rideout, *Classical Quantum Gravity* **25**, 065001 (2008).
 [37] J. Brunnemann and D. Rideout, *Classical Quantum Gravity* **25**, 065002 (2008).
 [38] E. Bianchi and H.M. Haggard, *Phys. Rev. D* **86**, 124010 (2012).

- [39] H. M. Haggard, [Phys. Rev. D **87**, 044020 \(2013\)](#).
- [40] D. M. Brink and G. R. Satchler, *Angular Momentum* (Clarendon Press, Oxford, 1968), 2nd ed.
- [41] E. Alesci and F. Cianfrani, [Phys. Rev. D **87**, 083521 \(2013\)](#).
- [42] E. Alesci and F. Cianfrani, [Europhys. Lett. **104**, 10001 \(2013\)](#).
- [43] E. Alesci and C. Rovelli, [Phys. Rev. D **76**, 104012 \(2007\)](#).
- [44] J. W. Barrett and L. Crane, [J. Math. Phys. \(N.Y.\) **39**, 3296 \(1998\)](#).
- [45] J. Engle, E. Livine, R. Pereira, and C. Rovelli, [Nucl. Phys. **B799**, 136 \(2008\)](#).
- [46] Wolfram Research, <http://functions.wolfram.com/HypergeometricFunctions/ThreeJSymbol/>.